Inhibition of Phosphoenolpyruvate Carboxykinase with a 3-Mercaptopicolinic acid Analogue

by

Matthew McLeod

A thesis

presented to the University of Waterloo

in fulfillment of the

thesis requirements for the degree of

Masters of Science

in

Biology

Waterloo, Ontario, Canada, 2016

Authors Declaration:

I hereby declare that I am the sole author of this thesis. This is a true copy of the thesis, including any required final revisions, as accepted by my examiners.

I understand that my thesis may be made electronically available to the public.

Abstract:

Phosphoenolpyruvate carboxykinase (PEPCK) is the metabolic enzyme that catalyzes the first committed step in gluconeogenesis and glyceroneogensis. More recently, PEPCK has been implicated in the maintenance and establishment of infections in macrophages by *Mycobacterium tuberculosis,* cancer cell growth and metabolic homeostasis, and overall TCA cycle flux as a moderator through removal of cycle anions. Many isoforms of PEPCK have been structurally and kinetically characterized against many different inhibitors. Of these inhibitors, 3-mercaptopincolinic acid (3-MPA) was shown to bind allosterically (K_i ~ 150µM) in an allosteric cleft behind the nucleotide binding pocket, as well competitively in the OAA/PEP binding site (K_i ~ 5µM). A new inhibitor, 3-carboxymethylthio-picolinic acid (CMP), has been designed based on of the structure of 3-MPA and other inhibitory studies by Stiffin *et al* (2009) in order to create a more selective inhibitor for PEPCK's active site. Previous studies mapping the active site of GTP-dependent PEPCKs has shown an overlapping secondary binding site adjacent to the competitive binding cleft. CMP has been designed from the previous 3-MPA molecule scaffold but with a simple carboxymethyl tail modification to simultaneously occupy the overlapping site. This study will investigate the structural and kinetic repercussions of the binding of CMP to three isozymes of PEPCK; PEPCK from *Mycobacterium tuberculosis*, rat cytosolic PEPCK, and finally human mitochondrial PEPCK. The data from the structural crystallographic studies of CMP and rat cytosolic PEPCK, it is shown that CMP does in fact occupy both the competitive site in coordination with the manganese ion but also extends into the overlapping adjacent pocket as intended. The kinetic results of CMP against the three isozymes in the catalytic direction of

PEP production shows an K_i ~ 30-90uM. These two results furthermore show that the adjacent binding cleft can be utilized for future, more selective, inhibition of GTP-dependent PEPCK.

Acknowledgements:

I would like to start off thank my family, Karen and Art McLeod and my brother Mike. Without their teaching and dedication to my growth I would not be in the position that I am today.

Thank you to Will Lotosky for introducing me into the lab during my undergraduate degree and fostering my drive for knowledge and understanding. Thanks to Marcia Chaudet for being a great resource when helping me with all structural biology related problems, and staying up late collecting data. Thanks to Iain Wallace and the rest of the Holyoak lab members, past and present, for keeping me sane and allowing me to truly enjoy my experience through my Masters. Thank you to all of my friends and colleagues I have gained through my time at grad school, I will cherish the memories we have created. Thank you to both Dr. Brendan McConkey and Dr. David Rose for guidance and help throughout my degree, as well as being a part of my committee.

Finally, thank you to Dr. Todd Holyoak. You're mentoring and fostering of me has allowed me to become the scientist I am today.

Table of Contents

List of Figures

List of Tables

List of Equations

List of Abbreviations:

PEPCK – Phosphoenolpyruvate carboxykinase

rcPEPCK – Rat cytosolic Phosphoenolpyruvate carboxykinase

hmPEPCK – Human mitochondrial Phosphoenolpyruvate carboxykinase

mtPEPCK – *Mycobacterium tuberculosis* Phosphoenolpyruvate carboxykinase

GTP – Guanosine-5'- triphosphate

GDP – Guanosine-5'- diphosphate

ATP – Adenosine-5'- triphosphate

3-MPA – 3-Mercaptopicolinic acid

CMP – 3-carboxymethyl-thio-picolinic acid

DTT – 1,4-dithiothreitol

TCEP – Tris-2-carboxyethyl-phosphine

OAA – Oxaloacetic acid

PEP – Phosphoenolpyruvate

IPTG – Isopropyl β-D-1-thiogalactopyranoside

βSP – 3-Sulfopyruvate

HEPES – 4-(2-hydroxyethyl)-1-poperazineethanesulfonic acid

ITP – Inosine-5'- triphosphate

PEG – Polyethylene glycol

TCA – Tricarboxylic acid cycle

Introduction - Part 1: Isozymes of PEPCK

1.1: History and Characterization of Phosphoenolpyruvate carboxykinase

The story of Phosphoenolpyruvate carboxykinase (PEPCK) was started in the 1950's with Utter and Kurahashi from Case Western University where they initially characterized the enzyme which they named oxaloacetate carboxylase.[62] In Utter and Kurahashi's mini-series, they outlined and documented PEPCK's nucleotide requirement as well as some mechanistic features of the catalysis of the enzyme, mainly the decarboxylation and subsequent phosphorylation of oxaloacetic acid (OAA) to form carbon dioxide and phosphoenolpyruvate.[62] From these mechanistic findings an entire subsect of enzymology and metabolomics with regards to PEPCK has been created, led by the late Dr. Richard Hanson. From the identification of PEPCK until now, a great deal is understood behind the reaction mechanism and requirements of various PEPCK isozymes. Even with 70 years of research focused on PEPCK, there may be a misunderstanding and underappreciated role of PEPCK in general TCA cycle flux/metabolism that has only recently begun to be elucidated.

1.2: Nucleotide Specificity

Referring back to Utter and Kurahashi, they determined that PEPCK purified from chicken liver had a nucleotide specificity of both ATP and/or ITP, although it is now known that chicken

PEPCK is GTP-dependent isozyme.[62] From this initial groundwork, it was determined that PEPCK has a nucleotide specificity where it can utilize either ATP or GTP, but not both. ITP, a third nucleotide triphosphate, can be substituted for GTP because of its pyrimidine ring carbonyl group coordinating with backbone amines of asparagine and phenylalanine in the active site. The structural differences between the two nucleotide specific classes of PEPCK can be seen within their respective nucleotide binding pockets. Figure 1.1 shows a structural alignment of the nucleotide binding cleft from submitted crystallographic structures from *Escherichia coli* (ATP-dependent) and *Rattus norvegicus* (GTP-dependent). In conjunction with this alignment, Figures 2 and 3 show the GTP and ATP binding pockets with their nucleotides bound. Finally Figure 4 shows the binding schematics from the crystallographic structures, highlighting distinct interacting residues. Recently, an inorganic pyrophosphate utilizing PEPCK was characterized from the parasite *Entamoeba histolytica*.[11] More work must be done to being to make conclusions about evolutionary phylogeny, and mechanistic properties of the unique pyrophosphate PEPCK.

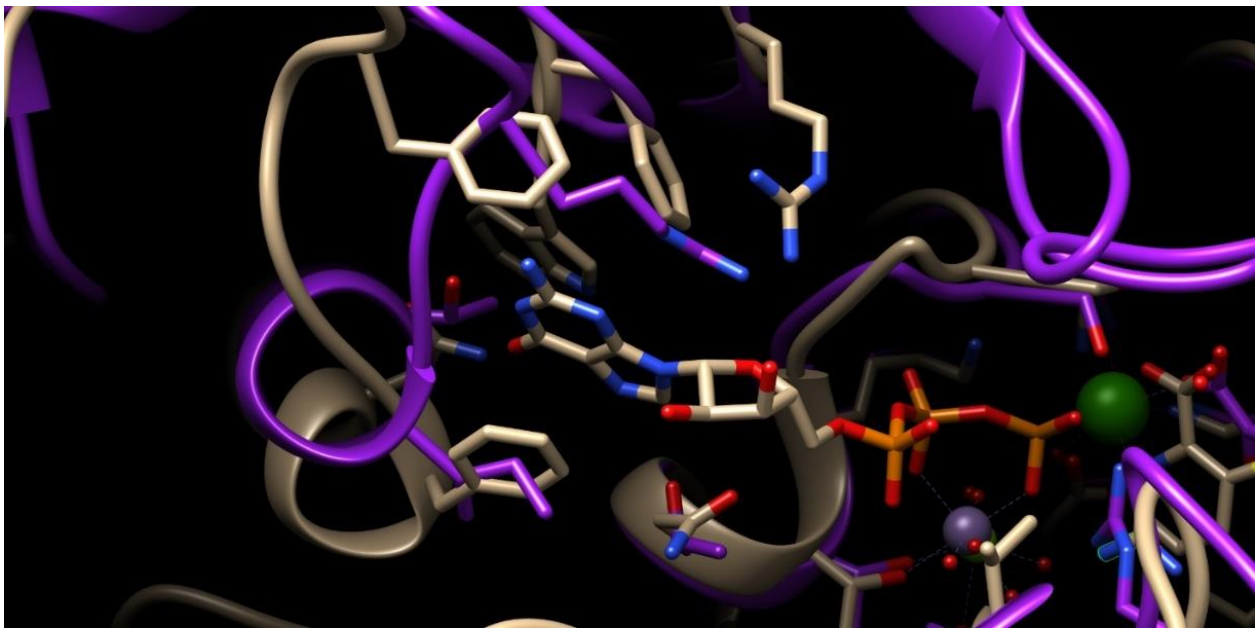

Figure 1.1: A*lignment of PDB ID 1OS1 (purple/Escherichia coli) and 4WY9 (tan/Rattus norvegicus). As seen, there are major differences in the overall architecture of the nucleotide binding pocket of GTP and ATP dependent isozymes. Figure is coloured by atom type, oxygen (red), nitrogen (blue), phosphorous (orange), magnesium (light green), manganese (dark green).*

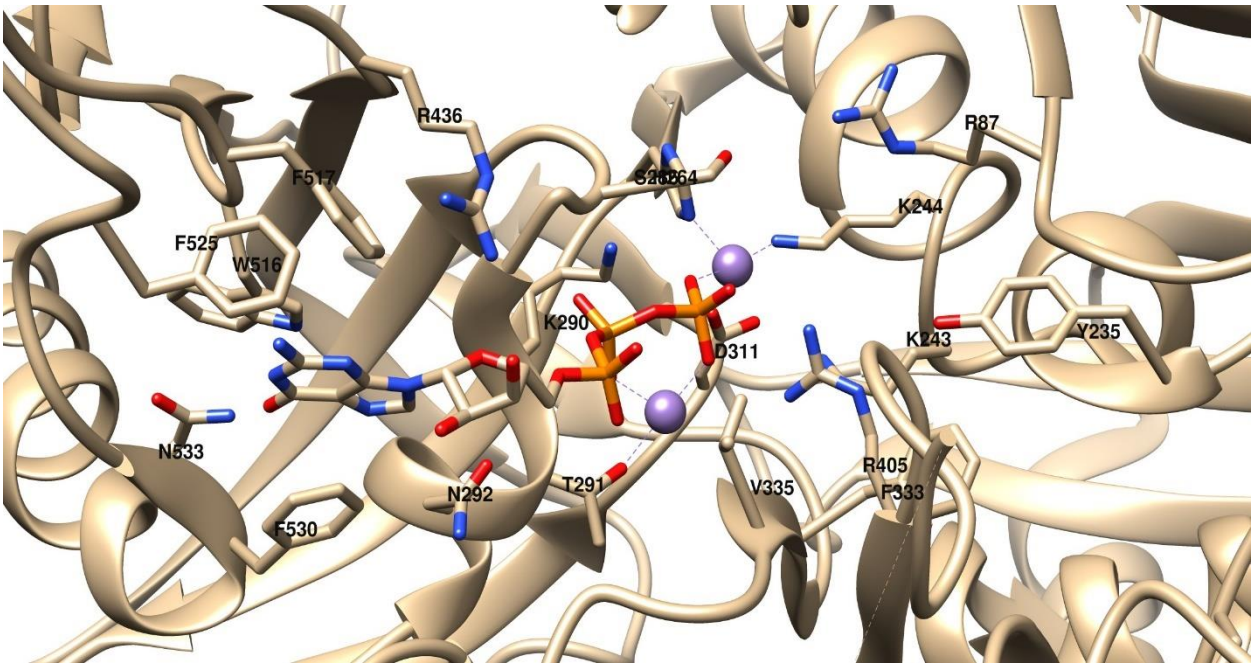

Figure 1.2: GTP binding pocket of Rattus norvegicus PEPCK with GTP bound. The image was generated from PDB ID#4YW9. Purple atoms are manganese. Residues labelled are all residues interacting with the nucleotide.

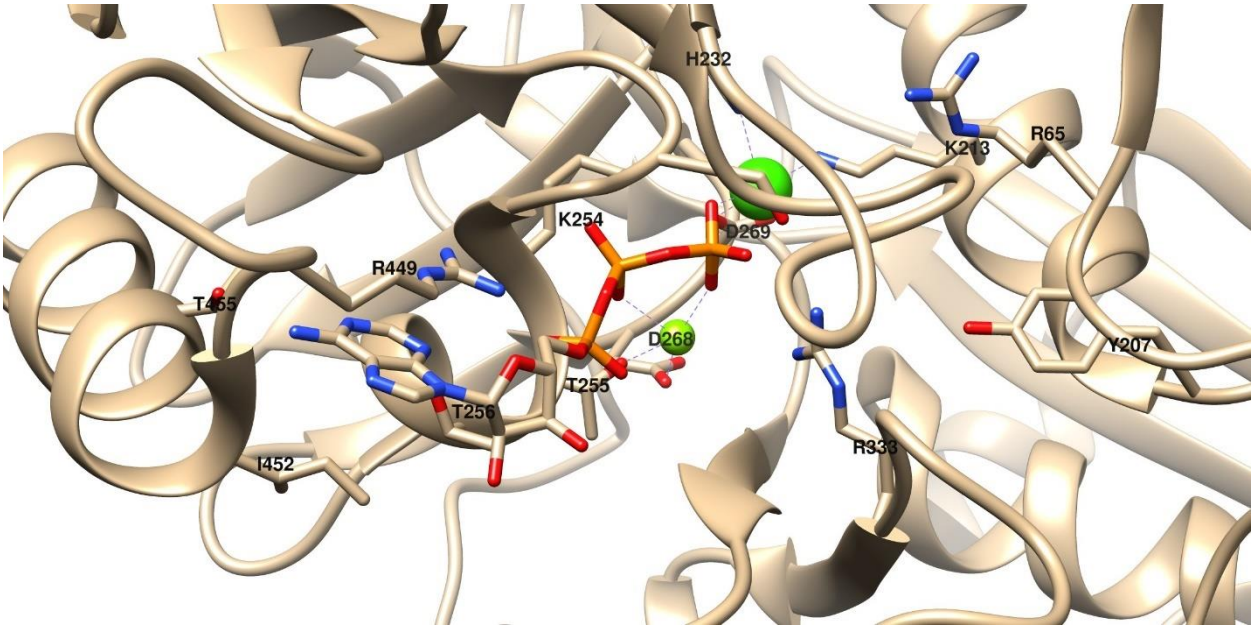

Figure 1.3: ATP binding pocket of Escherichia coli PEPCK with ATP bound. The image was generated from PDB ID#1OS1. Residues labelled are all residues interacting with the nucleotide. The green atoms indicate calcium ions.

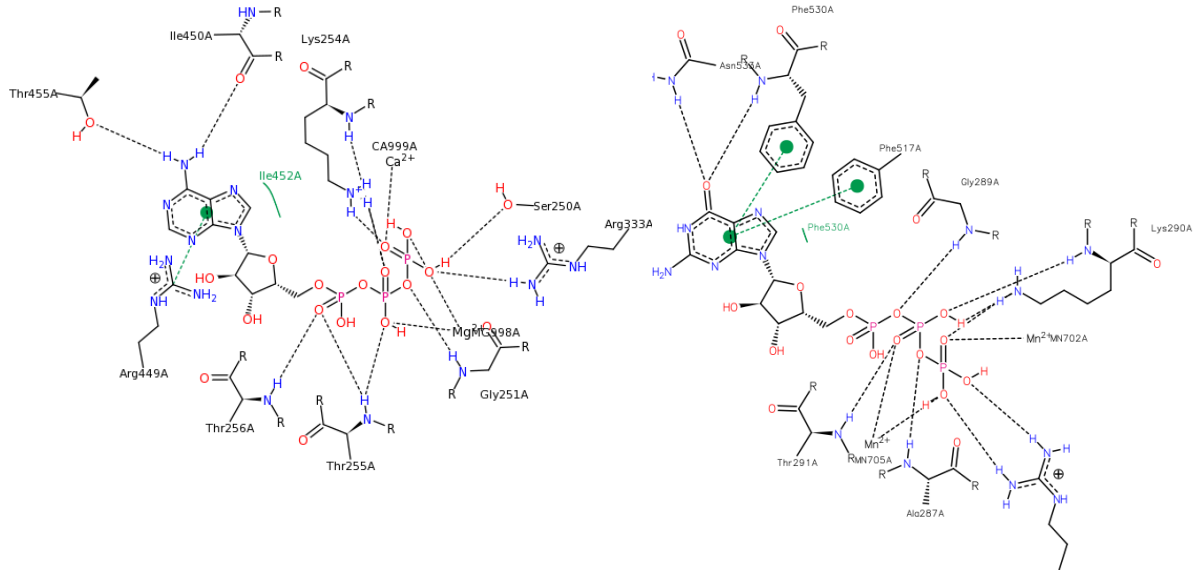

Figure 1.4: Binding schematic for nucleotide binding site A) ATP- B) GTP-dependent PEPCK. ATP binding cleft of Escherichia coli (PDB ID#1OS1). Figure 2B represents the binding schematic for GTP in nucleotide cleft of Rattus norvegicus (PDB ID#4YW9)

1.3: Compartmental Specificity

A comprehensive review from Hanson and Garber (1972) recap work done by many different research groups highlighting the isozymes of PEPCK.[20] Chang *et al* (1966) initially purified mitochondrial PEPCK which has a similar molecular weight as the cytosolic isoform that Ballard and Hanson purified three year later. [5,10] This solidified the idea that PEPCK exists in higher order mammals as compartmental isozymes, both mitochondrial and cytosolic. The role and implications of having two compartmental isozymes in higher mammals is still under investigation because of a lack of biochemical analysis of the mitochondrial isozyme. This lack of information is a result of organismal differences in the distribution of the two compartmental distinct isozymes. Referring to Table 1.1 it can be seen there is large variability in this relative distribution, while the traditional mouse model has a much greater amount of cytosolic PEPCK in relation to the mitochondrial isozyme.[20] To further impact this distribution problem, different tissues within an organism can have different ratios of compartmental PEPCK.[20] To date, one theory is that mitochondrial PEPCK maintains redox balance by forgoing transport of reducing equivalents across the mitochondrial membrane, by participating in lactic acid metabolism. Lactate is a common by-product of sustained physical activity. Birds, which typically undergo longer periods of labourous physical activity have >90% abundance of mitochondrial PEPCK.[20] The interplay between the two distinct compartmental isozymes has not been fully clarified. In knock out studies using a mouse model, global ablation of cytosolic PEPCK caused major citric acid cycle flux dysregulation and eventual death.[18] Mendes-Lucas *et al* created a second rat strain in which cytosolic PEPCK was knocked out, but mitochondrial PEPCK was overexpressed to physiologically relevant levels of the cytosolic isozyme. The result

was incomplete reestablishment of metabolic homeostasis. This was interpreted as the compartmental isozymes having independent control over citric acid cycle flux and PEP production.[38]

Table 1: Activity distribution of total PEPCK separated into compartmental isozymes in various different organisms from Hanson & Garbers review.

Distribution of PEPCK Isozymes Across Different Species

Species	Mitochondrial	Cytosolic
Human	60	40
Guinea pig	60	40
Cow	50	50
Sheep	35	65
Cat	65	35
Hamster	5	95
Rat	10	90
Mouse	10	90
Rabbit	95	5
Pigeon	95	5

1.4: The Gene Loci of Compartmental Isozymes

As highlighted above, the two compartmental isozymes found within higher order mammals although indistinct in their catalysis have unique distributions across species. Interestingly, these two homologous genes are found on two different chromosomes, and are under different regulatory control. Cytosolic PEPCK is found on chromosome 14, while the mitochondrial form is found on chromosome 20.[40] This further reinforces the idea that these two isozymes function independently.

Introduction – Part 2: Regulation and Expression

2.1: Lysine Acetylation

More recently, cytosolic PEPCK has been shown to be susceptible to post-translational modifications through lysine acetylation which has a direct impact on PEPCK at an enzymatic level.[23,34] Increased acetylation caused increase interactions with UBR5 ubiquitin ligase, leading to ubiquitination and subsequent recycling of PEPCK by the proteasome.[23] Lysine acetylation is the only known post-translational modification that regulates cytosolic PEPCK, all other regulation is at the genomic level. In March of 2016, a new study investigated Sirt2, a deacetylase determined to be specific for PEPCK by the Jiang 2011 study. It was found that Sirt2 has no interaction with the acetylated lysines of PEPCK, highlighting a need for more studies to elucidate lysine acetylation as a regulatory mechanism of PEPCK and raising the question if lysine acetylation is indeed a mechanism of PEPCK regulation *in vivo*.[28]

2.2: Hormonal & Small Molecule Control

PEPCK's role within metabolic homeostasis as a whole implies a tight control over its expression and regulation. There has been an influx of recent work investigating the regulation of these enzymes. It appears that the general consensus is each tissue reacts differently to various regulators of PEPCK expression. PEPCK's regulation of expression of starts during development, where PEPCK must be upregulated for the newborn to survive in the early stages of infancy.[3] Total knockout studies showed that mice without PEPCK were severely hypoglycemic eventually

resulting in death.[49] Most of the regulation of PEPCK has been focused on the cytosolic isozyme, although there are distinct differences in the expression of the cytosolic and mitochondrial isozymes. For example, the cytosolic isozyme has a half life of 6 hours and is environmentally/hormonal regulated, while the mitochondrial isoform is constitutively expressed with a half life of 60 hours.[60] Hanson and colleagues did a review on the regulation of cytosolic PEPCK, and the general result is that the gene is tightly regulated by a plethora of variables on a transcriptional level, such as cAMP, glucocorticoids, and pH/metabolic acidosis (Figure 2.1).[12,27,44]

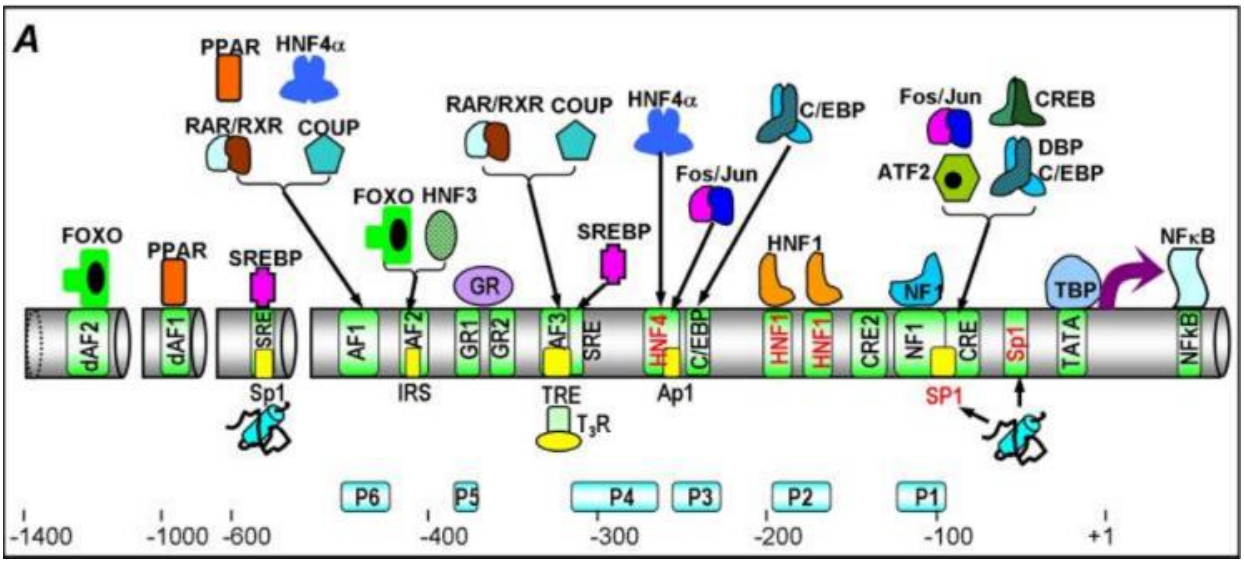

Figure 2.1: Cytosolic PEPCK gene from Yang et al 2009 review. Highlights all regulatory elements of the gene on various loci. The yellow regions are overlapping binding sites for various regulators.

This image/research was originally published in The Journal of Biological Chemistry. Yang, J., Reshef, L., Cassuto, H., Aleman, G., & Hanson, RW. Aspects of the Control of Phosphoenolpyruvate Carboxykinase Gene Transcription. The Journal of Biological Chemistry. 2009. 284: 27031-27035. © the American Society for Biochemistry and Molecular Biology.

These modifiers include cAMP, a marker of higher metabolic requirements, where administration causes a 5-8 fold increase in mRNA within 20 minutes.[29] This phenomenon was followed by a marked decrease in PEPCK mRNA levels, which was attributed to a reflexive glucocorticoid response inducing insulin secretion.[29] The effect of insulin on transcription levels was further reinforced a year later when Granner and his colleagues showed insulin, at physiologically relevant concentrations, inhibits transcription of PCK1, the gene of the cytosolic PEPCK.[17] The most recent publication from Seenappa *et al* showed that Genistein, a soy bean isoflavone, acts by destabilizing cytosolic PEPCK mRNA, leading to decrease activity of the enzyme.[48] There is very little regulation directly on PEPCK's activity, with administration of Bt_2cAMP causing an acute 3-fold increases in activity.[46]

2.3: Methylation

Benvenisty *et al* (1985) investigated the tissue specific methylation of PCK1 and found that there is a correlation with decreased methylation of PEPCK and increased rates of transcription.[16] Along with gene methylation, the histones associated with PCK1 chromatin have shown to be regulated through arginine methylation. Insulin was shown to stimulate a 2.5-fold increase in histone H3 dimethylation, indicating a decrease in transcription.[19]

2.4: DNAse 1 Hypersensitivity

Many groups have investigated various DNase 1 hypersensitive regions along the gene promoter region for PEPCK. The DNase 1 hypersensitive sites are hallmark regulatory gene sequences that denote actively transcribed genes as they are revealed once chromatin remodelling occurs. They also indicate tissue specific regulation, as particular hypersensitive sites are found only in one tissue, for example site A (-4800bp) being liver specific.[66] This finding further reinforces differential PCK1 gene expression in tissues.

Introduction – Part 3: Metabolic Function and Biomedical Implications

3.1: Functional Role

Even though PEPCK has been studied for 70 years, the functional role of this enzyme in metabolism is still misunderstood. When parsing through textbooks PEPCK is solely referred to as a gluconeogenic enzyme. Although its catalysis marks the first committed step in gluconeogenesis, this is not the only role of PEPCK. PEPCK's has a cataplerotic function for the citric acid cycle, by removing intermediates.

3.2: The Citric Acid Cycle

The citric acid cycle is an aerobic metabolic process in the mitochondria that recycles acetyl-CoA through conversion into various intermediates. Acetyl-CoA is originally obtained through various processes from substrates that include amino acids, carbohydrates, and lipids. Each turn of the cycle yields 3 $NADH_2$, 1 $FADH_2$, and 1 GTP molecule.[1] PEPCK acts by removing citric acid anions, as oxaloacetate, for the conversion of PEP.[1] In this, PEPCK acts as a moderator of the citric acid cycle by maintaining a constant flux. PEP can then be used for a variety of functions required for the cell, from biosynthesis of serine and small amino acids, to the production of glycerol for glyceroneogenesis. PEPCK flux to create PEP can also feed back into the citric acid cycle by creating acetyl-CoA through pyruvate synthesis and subsequent oxidation (Figure 6). These functional roles of PEPCK show themselves very clearly with recent literature highlighting various medical maladies and PEPCK's role in them. [14,15,31,36,39,64,67]

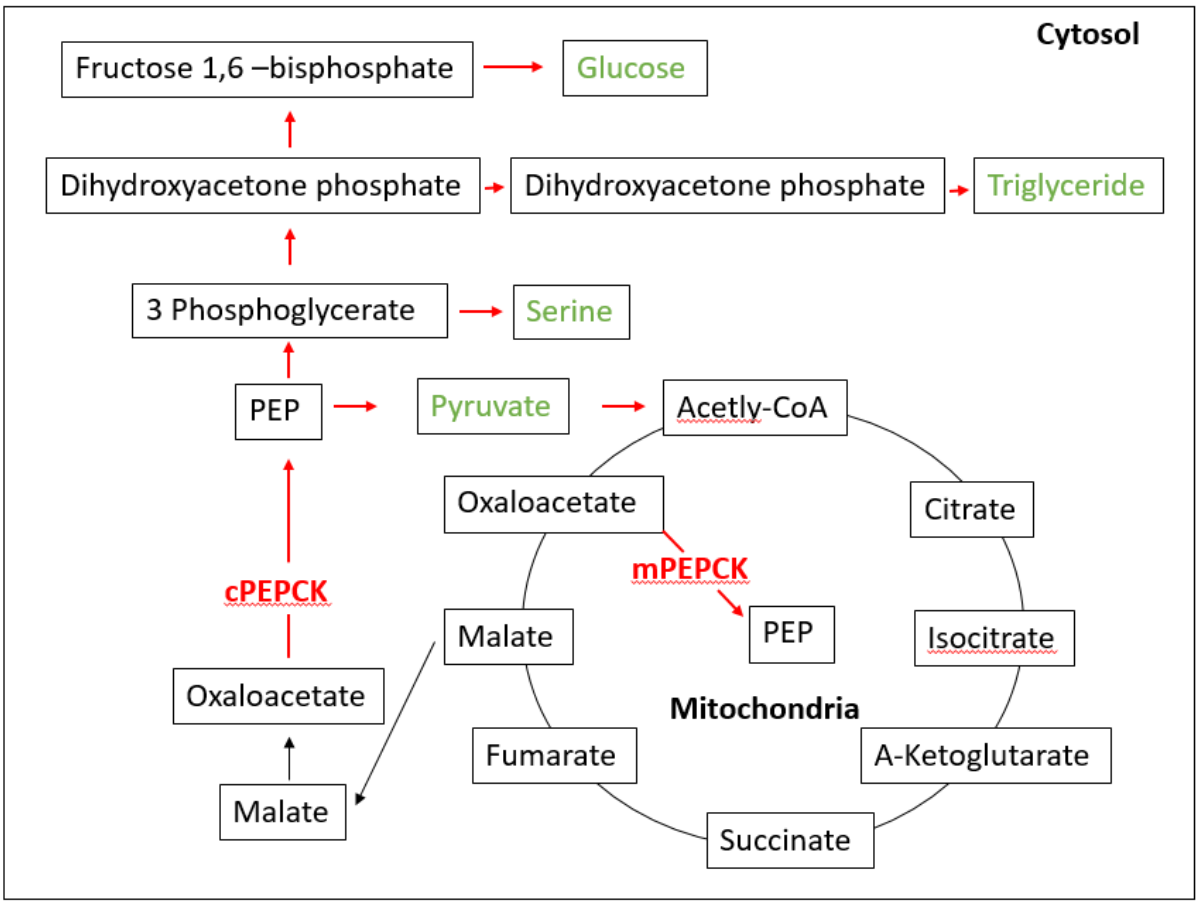

Figure 3.1: Schematic representation adapted from Yang, Kalhan, and Hanson review. Indicates where compartmental isozymes function with regards to the TCA cycle, and the various outcomes of PEP.

3.3: Diabetes and Glucose Homeostasis

Diabetes and dysregulation of glucose homeostasis has been the primary medical ailment related to PEPCK because of its function in gluconeogenesis. Besides PEPCK's role in glucose production, a new role of the mitochondrial enzyme has been elucidated. Insulin secretion was initially thought to be solely coupled with the generation of ATP in beta islet cells.[52] In this model, as glycolysis and the TCA cycle turnover, ATP is generated creating a higher ratio of ATP/ADP. This influx of ATP causes K_{ATP} voltage gated channels to open, creating depolarization and release of insulin.[52] Mice with this K_{ATP} channel knocked out still have glucose stimulated insulin secretion (GSIS), showing this isn't the only mechanism for insulin secretion.[59] Stark and his colleagues recently found a correlation with mitochondrial PEPCK flux and GSIS. It was proposed that mitochondrial GTP (mtGTP), produced by GTP dependent - succinyl CoA synthase (SCS-GTP) is a metric for TCA cycle flux.[53] PEPCK utilizes mtGTP to produce PEP which has been proposed to induce insulin secretion.[56]

Many groups have done knockout studies in mice to determine the role of PEPCK in gluconeogenesis, and therefore diabetes. Stark and her colleagues investigated mitochondrial PEPCK via silencing. They found these deficient mice had lower plasma glucose, triacylglycerides, fat mass, with raised lactate levels.[51] This silencing hindered gluconeogenesis, but it appeared that the cytosolic isoform had partial compensation.[51] The overall effect on homeostasis may be quite different in organisms with different distribution of the two isoforms.[51]

Many studies with cytosolic PEPCK knock outs have been completed. These studies show the ability for the kidney to take over gluconeogenic function from hepatic knockouts.[49] But whole body knock outs resulted in hypoglycemia and death of the mice in approximately 2 days.[49] Other studies indicated that PEPCK's role is not solely gluconeogenic. One such knock out study with hepatic cytosolic knock out mice resulted in extremely fatty livers. Hakimi *et al* showed that this lipid deposition indicates that cytosolic PEPCK isn't only involved with gluconeogenesis. There conclusion was that without cytosolic PEPCK, major TCA and mitochondrial dysfunction occurred.[7,18]

3.4: Metabolic Function – *Mycobacterium tuberculosis* Infections

Early in 2010, a new link between *Mycobacterium tuberculosis* infection and PEPCK was established. Marrero *et al*, with the knowledge that *M. tuberculosis* utilize fats as a primary carbon source, target PEPCK to see the effect of various knock outs and silencing. They found that *M. tuberculosis* strains deficient in PEPCK could not establish infections in macrophages or mice hosts.[36] Secondly, *M. tuberculosis* that had already established a chronic infection required PEPCK for persistence. Silencing of PEPCK resulted in the clearance of the infection.[36] These findings show a potential therapeutic target for the treatment of multi-drug resistant tuberculosis infections.

3.5: Metabolic Function – Cancer

In 2014, an initial paper relating mitochondrial PEPCK to cancer was released by Mendez-Lucas and his colleagues.[39] Since then, a flurry of papers investigating this relationship has come to light. Cancer cells have adopted a unique metabolism that is specialized to the particular cancer type, but it has allowed these cells to be highly adaptive to their environment. Mendez-Lucas first initially showed that PCK2, the gene for mitochondrial PEPCK, was upregulated in many stress pathways that cancer cells typically utilize for survival.[38] Li and her colleagues started the influx of insight into cancer metabolism of PEPCK, with a first conclusion that PCK1 is upregulated in stem-cell like cancer cells, and possibly undifferentiated cells.[33]

In 1925, Otto Warburg came to the conclusion that cancer cells adopt a unique metabolism where they undergo aerobic glycolysis.[65] This metabolism will greatly utilize glucose to have high glycolytic flux. In the end of glycolysis, PEP is catalyzed by pyruvate kinase to yield pyruvate, which feeds into the TCA cycle. A new theory proposed by Vincent *et al* (2015) is that once glucose is consumed in the tumor microenvironment, cancer cells will change their metabolism and focus flux through PEPCK, thus filling the high demand for PEP.[64] The lack of environmental glucose and change in primary metabolism leads to an upregulation of expression of mitochondrial PEPCK. This high flux may be attributed to a phenomena called glutamine addiction, where cancer cells utilize increased amount of glutamine.[15] This glutamine is converted into α-ketoglutarate which then fuels the TCA cycle.

PEPCK has also been implicated in chemoradiation susceptibility in colorectal cancer cell lines.[42] 5-Flurouracil is a common therapeutic agent that inhibits thymidylate synthase, an enzyme that

produces thymidine for DNA synthesis and replication. A link was found between downregulation of mitochondrial PEPCK and 5-Flurouracil resistance, although no clear mechanism was deduced.[42]

Finally, Leithner *et al* in 2014 showed inhibition of PEPCK through treatment of 3-mercaptopicolinic acid, or silencing of PCK2 by siRNA significantly increased apoptosis of various lung cancer cell lines. This increase in apoptosis occurred in glucose deprived environments, while it was ineffective in media where glucose was in excess.[31]

3.6: Metabolic Function – Aging

2016 has marked a new biomedical front for PEPCK, led by the late Dr. Hanson and his colleagues. Aging is a deeply studied phenomenon that has recently been linked to a change in metabolism. This change is away from aerobic metabolism, the utilization of the TCA cycle, to a mainly anaerobic glycolysis.[67] This shift to anaerobic glycolysis in only further exasperated by a general lack of physical activity and dietary changes. Hanson and his colleagues showed a reciprocal regulation between cytosolic PEPCK, and Pyruvate kinase (PK) in aging *C. elegans*. In aged *C. elegans*, PEPCK was downregulated effecting TCA cycle flux, while PK was upregulated increasing glycolytic flux.[67]

Introduction - Part 4: Enzyme Structure and Catalysis

4.1: Introduction to Catalysis

As mentioned before, many characterizations have been done with regard to the various isozymes of PEPCK; whether ATP vs GTP dependent enzymes, or mitochondrial vs cytosolic. These enzymes, having the same catalytic mechanism, have very similar active sites. In summary, all enzymes have a requirement for 2 divalent metal cations, substrate (either OAA for forward reaction, or PEP for reverse), and a nucleotide. Many studies have been completed investigating the dual cation requirements of PEPCK, and there seems to be preferential metal cation requirements for the various isozymes across different species. For instance, for chicken mitochondrial PEPCK, the most activating of the cations is one magnesium and one manganese ion, although iron or cobalt can substitute for manganese.[30] It is thought that the initial magnesium cation forms a Mn^{2+}-nucleotide complex that is activating for the enzyme, with the manganese for the basis for substrate binding in the active cleft.[41,50] All GTP-dependent PEPCK enzymes also have a similar molecular weight approximating 70kDa and exist as monomers, while some ATP-dependent PEPCK exist as functional multimers. The general mechanism of catalysis is as follows: OAA binds in octahedral coordination with metal cation in conjunction with nucleotide binding, decarboxylation of OAA to relinquish carbon dioxide and create a reactive enolate intermediate, phosphorylation of enolate by gamma-phosphate of nucleotide, and finally product release. Although most characterized PEPCK's favour decarboxylation of OAA, some isozymes carboxylate PEP to refill the TCA cycle. These enzymes are generally from parasitic eukaryotic sources.[13,14,43]

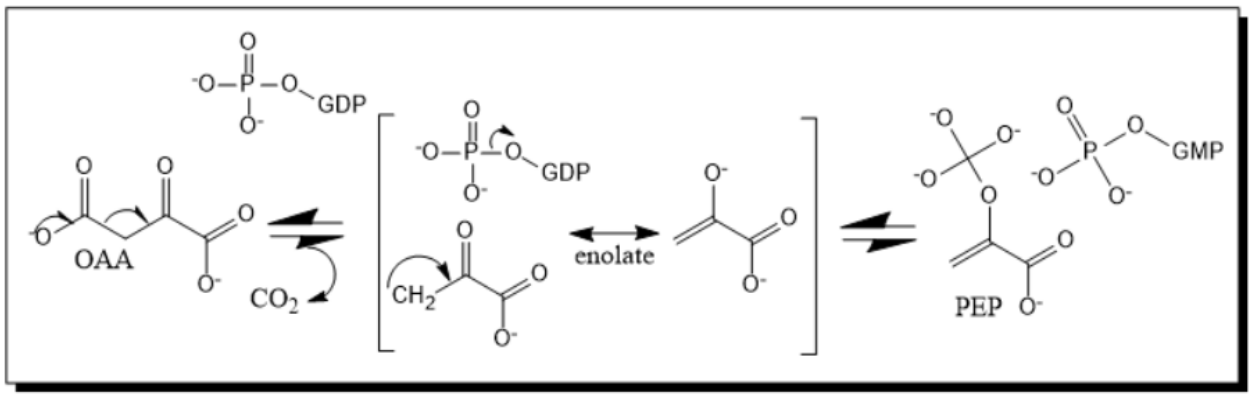

Figure 4.1: Reaction mechanism for the forward catalysis of OAA to PEP by PEPCK.

4.2: General Structural/Sequence Similarity

Structural work investigating the intricacies of PEPCK's catalysis has been completed across many different species. To date, there are 69 deposited structures with from various organisms such as; *Rattus norveigcus*, *Escherichia coli, Mycobacterium tuberculosis*, *Homo sapiens, Thermus thermophiles, Gallus gallus, Anaerobiospirillum succiniciproducens, Cornyebacterium glutamicum, Actinobacillus succinogenes*, and *Trypanosoma cruzi.* These structures include both ATP and GTP-dependent isoforms, as well as mitochondrial and cytosolic variants.

The overall sequence similarity between mitochondrial and cytosolic isozymes is above 60%, and the active site of ATP and GTP dependent isozymes are mostly conserved with the only differences located in the nucleotide binding cleft.[22] Structural comparison revealed their quaternary structures are well conserved between rat cytosolic and avian mitochondrial with a Cα RMSD value of 0.94 Å.[58] Finally there are no related protein families having related architecture to PEPCK, and therefore have been classified as their own PEPCK family (Pfam ID# PF00821).[16]

4.3: Gross Architecture of PEPCK

PEPCK has been categorized into two main domains; an N-terminal (residues 1-259), C-terminal (residues 160-622), and finally an active site placed in between the two termini. This categorization was first popularized by Matte, Goldie, Sweet, and Delbaere in their 1996 paper highlighting the structure of *Escherichia coli* ATP-dependent PEPCK, Figure 4.2.[37]

Matte and his colleagues determined that these two individual domains do not fold separately from one another, but rather they make many passes through one another.[36] These two domains undergo dynamic shifts during catalysis, where they rotate inwards towards the active site. This movement is proposed to reduce the volume of the active site, excluding solvent which can pronate the reactive intermediate to produce unfavourable pyruvate. This reduction in active site volume also forces the nucleotide and substrate closer to one another to position them for catalysis.[58]

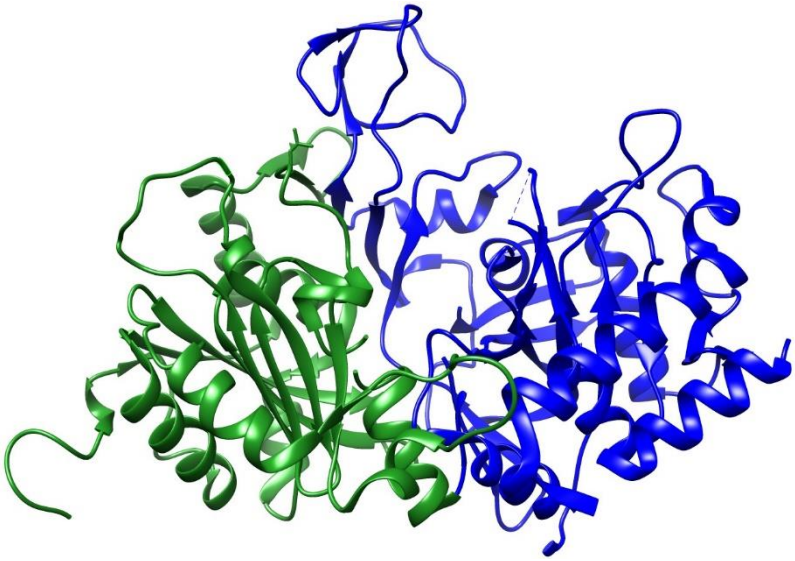

Figure 4.2: Two major domains of PEPCK. The N-terminal domain is in green from residues 1-259. The C-terminal domain is in blue from residues 260-622. Modelled enzyme is from GTP-dependent Rat cytosolic PEPCK.

4.4: Dynamic Mobile Motifs & Structural Characteristics

For the remainder of the thesis, rat cytosolic PEPCK will be used as a reference structure unless otherwise stated.

Since the initial structural characterization of Dunten in 2002 of the human cytosolic enzyme, 3 major mobile motifs have been identified and relatively conserved in PEPCK. These motifs undergo conformation changes from open-closed state that aligned substrates into coordination that allow for catalysis (Figure 4.3).

The first of these dynamic elements is the R Loop, residues 85-92, which appears to interact directly with OAA. A secondary purpose of the R-loop is its interaction with the Omega loop. This is the contact that is believed to allow for the "locking" of the omega loop over the active site.[25]

Secondly, the P-loop is the most characterized mobile element in the active site of PEPCK. This P(hosphate)-loop is kinase-1a motif, which is a common structural element in binding phosphate/nucleotide binding.[61] The P-loop spans residues 284-292 and is responsible for cradling the β and γ phosphates. Its rotation into a closed state brings the nucleotide triphosphate towards the M1 metal, bridging both cations together. This movement allows for phosphoryl transfer onto the intermediate. The conformation change to a closed state upon nucleotide binding also relieves a steric clash between A287 of the P-loop and T465 of the omega loop. S286 of the P-loop has a function in substrate binding, as it interacts with O5 of OAA.[58] The P-loop also contains a completely conserved cysteine, C288, that has been shown to

result in inactivation of the enzyme if altered. This alteration could be pH dependent, sulfhydration, or other factors.[32,62]

The final mobile element is an omega loop, which is ~10 amino acids from residues 464-474, that resemble the omega symbol. This motif acts as a lid over the active site. Once the Michaelis-Menten complex has formed, the loop will close to prevent unwanted protonation of the reaction intermediate from bulk solvent. The omega-loop has a functional role of maintain the bi-lobal motion of the C- and N-terminal domains after they have rotated inward in the catalytically competent conformer.[25] Only once the omega-loop has sampled the closed conformation are the substrates in an orientation that allows catalysis to occur.[25]

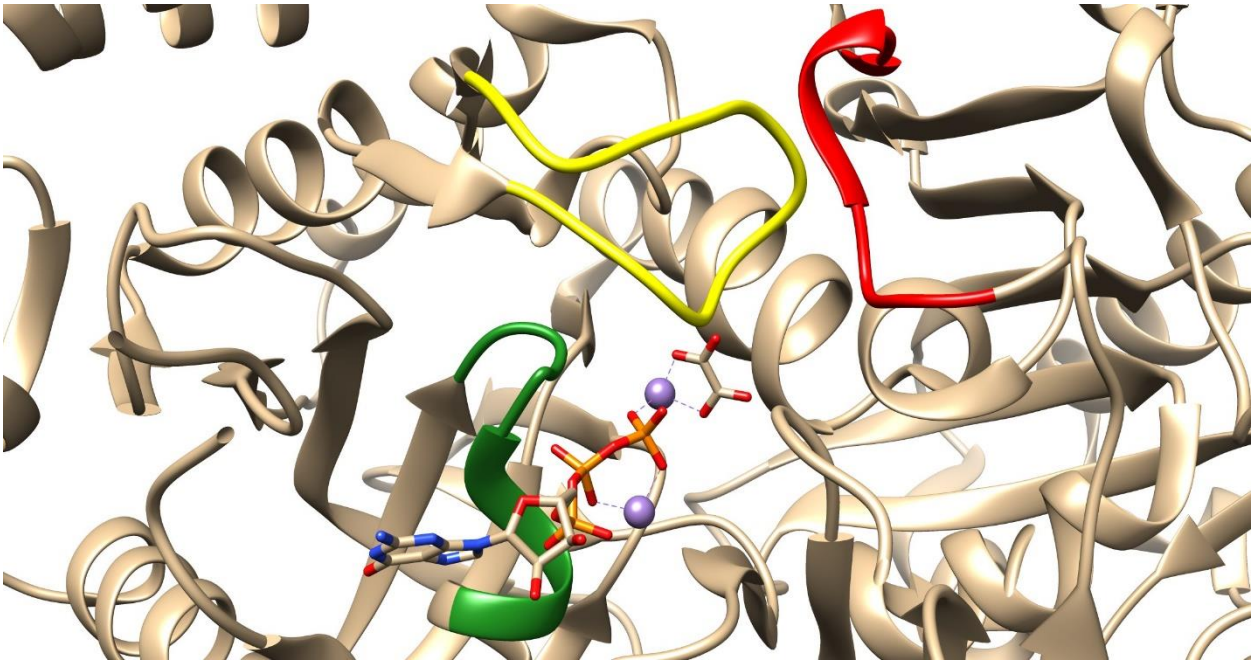

Figure 4.3: Various dynamic motifs of PEPCK's active site highlighting the R-loop (red), P-loop (green), Omega-loop (yellow). This structure was generated from the PDB ID#3DT2, a complex of rat cytosolic PEPCK with GTP and oxalate.

Introduction – Part 5: Catalysis and Reaction Mechanism

5.1: The Holo-Enzyme of PEPCK

PEPCK's initial state prior to substrate binding is an open conformation with one of the two divalent metal cation required for catalysis bound to the active site. The manganese is in an octahedral conformation in coordination with K244, H264, D311, and various water molecules to fill the rest of the occupancies (Figure 5.1).[57] In the chicken mitochondrial isozyme, the reactive cysteine C307 (C288 in rat cytosolic PEPCK) can be shown interacting with the active site manganese in a tetrahedral conformation but this geometry is not seen in the rat cytosolic PEPCK.[22] This tetrahedral geometry may represent the basis of some level of regulation, and may give insight into differing kinetic effects when the M1 manganese is substituted with other metals.[22]

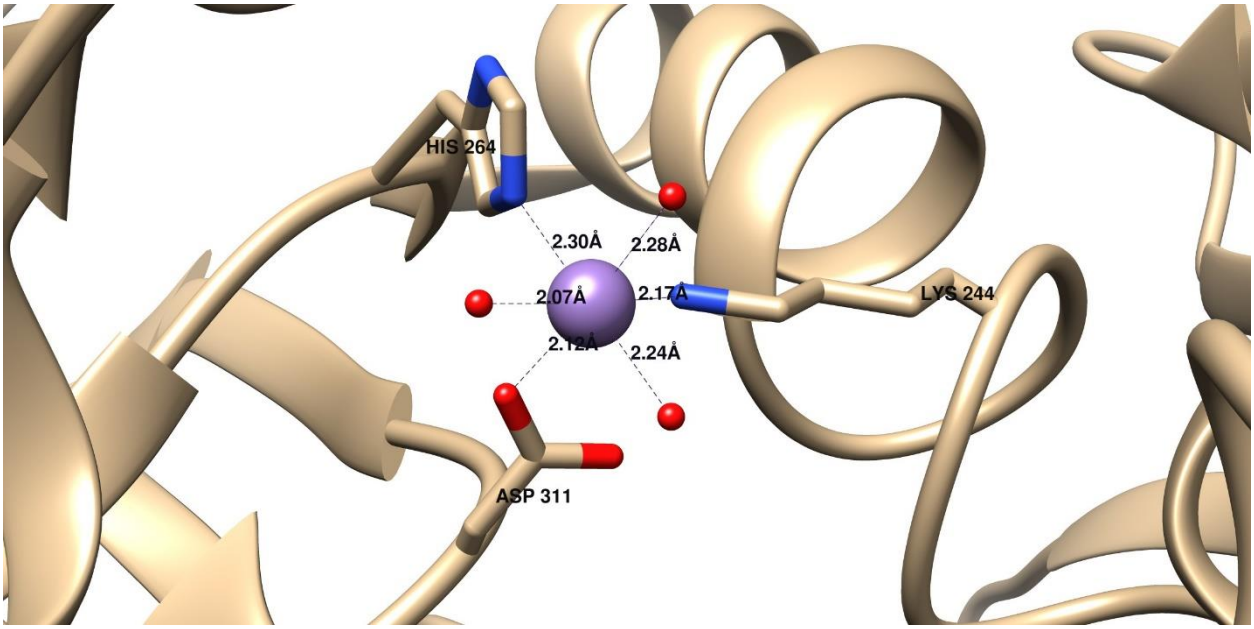

Figure 5.1: Manganese M1 meta (purple)l bound in octahedral coordination from PDB ID# 2QEW. All bonding residues; H265, K244, and D311 holding manganese in place, are highlighted.

5.2: Binding of Substrates – R-loop & OAA

For catalysis to occur, the 3 dynamic motifs must undergo a shift from an open unordered state to a closed ordered state. For this to occur, the nucleotide substrate as well as OAA/PEP must bind. OAA binds with the M1 metal in two conformations, one that does not allow for catalysis to occur, while the other is the competent orientation (Figure 5.2 and 5.3).[57] The proper orientation positions OAA O3 and O5 coordinated with M1. O5 also interacts with the P-loop S286 while O4 interacts with R87 of the R-loop.[57] In this state, O2 of OAA interacts again with R87's Nε (Figure 5.2).[57]

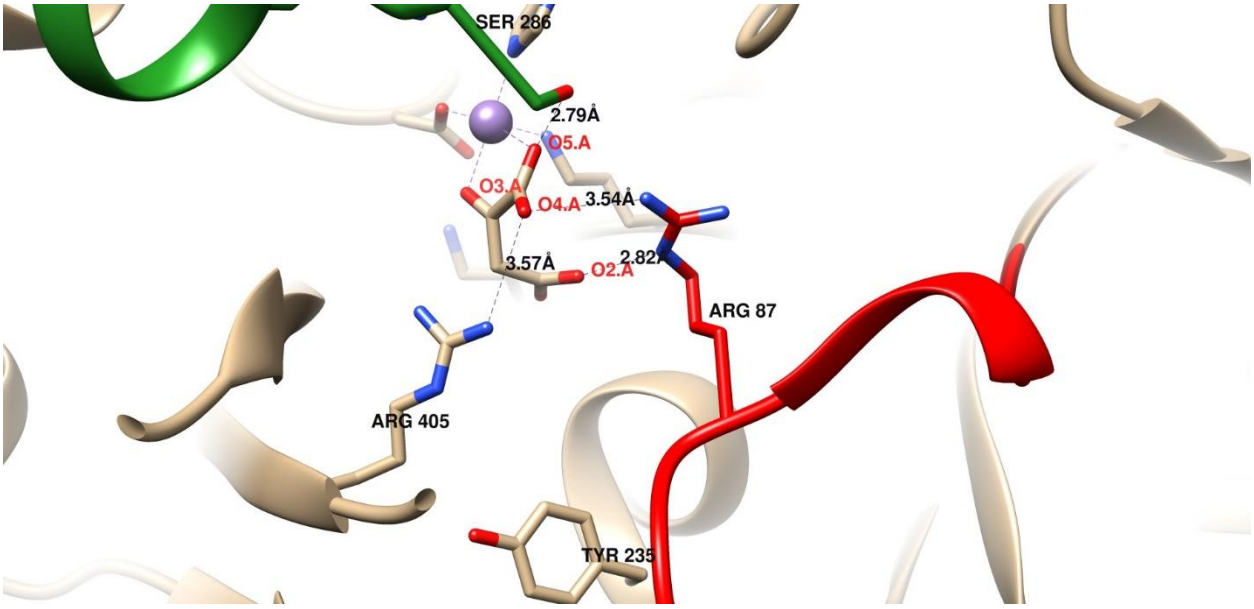

Figure 5.2: OAA bound to M1 in catalytically competent orientation from PDB ID#2QF2. P Loop (green) and R Loop (red) are labelled.

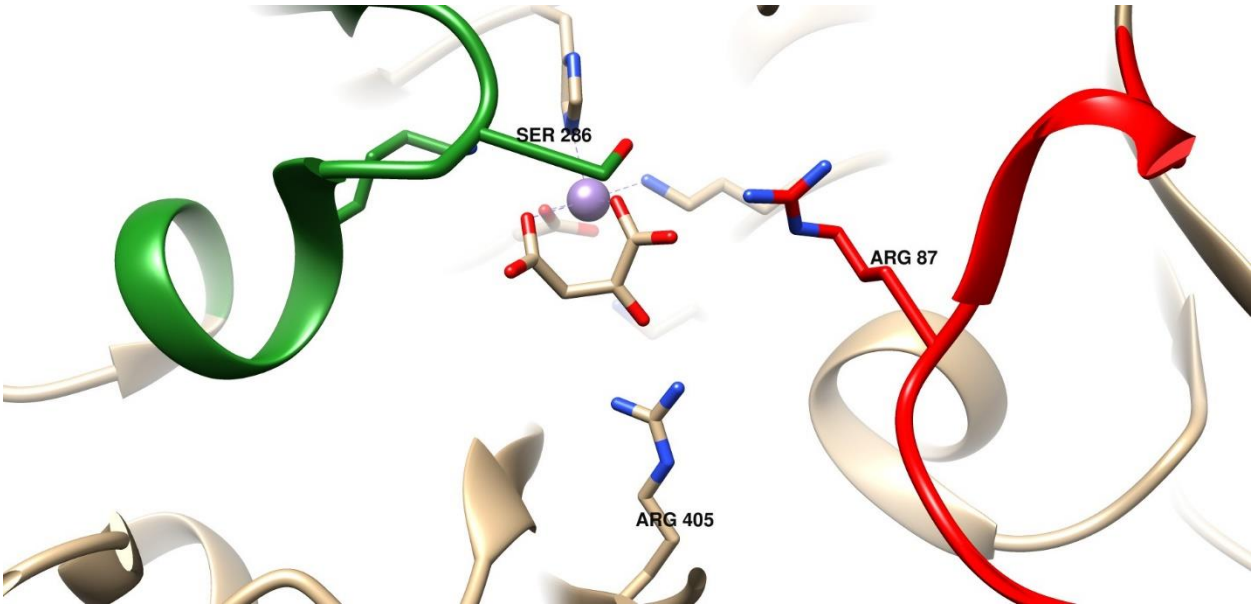

Figure 5.3: OAA bound to M1 in catalytically incompetent conformation from PDB ID#2QF2. P Loop (green) and R Loop (red) are labelled.

5.3: Binding of Substrates – P-Loop & GTP

GTP's guanosine base interacts in the nucleotide binding pocket through pi-stacking of Phe530 and 517 and hydrogen bonding of Asn533 with the carbonyl O6 (Figure 5.4).[5] The nucleotide binds to the M2 metal which supports the γ and β phosphates. The M2 cation is stabilized in the active site by T291 (P-loop), while water molecules occupy the rest of the octahedral coordination (Figure 5.5).[57] The P-loop when in ordered orientation, specifically T291 and G289, stabilizes the 3 phosphates which brings the nucleotide into proximity to M1 and OAA.[57] The 3 phosphate groups are orientated in an eclipsed orientation which increases the energy state of GTP.[57] This allows for phosphoryl transfer to happen more readily.

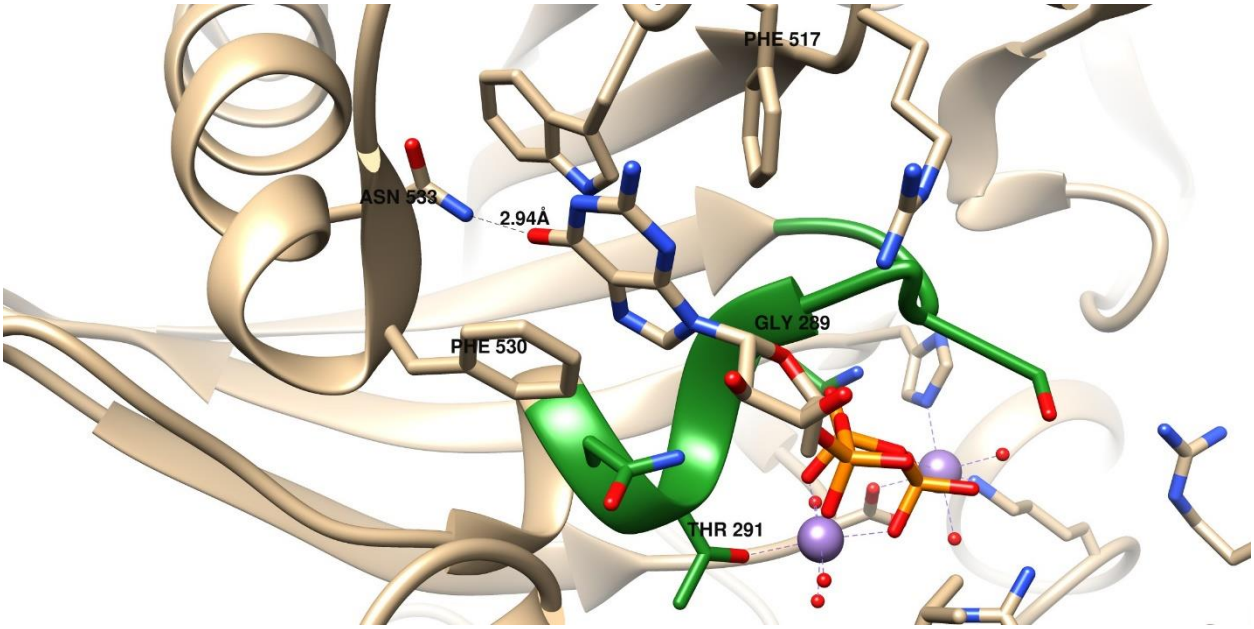

Figure 5.4: GTP-nucleotide binding pocket with GTP bound from PDB ID#2QEY. All contacting residues and P Loop (green) are labelled.

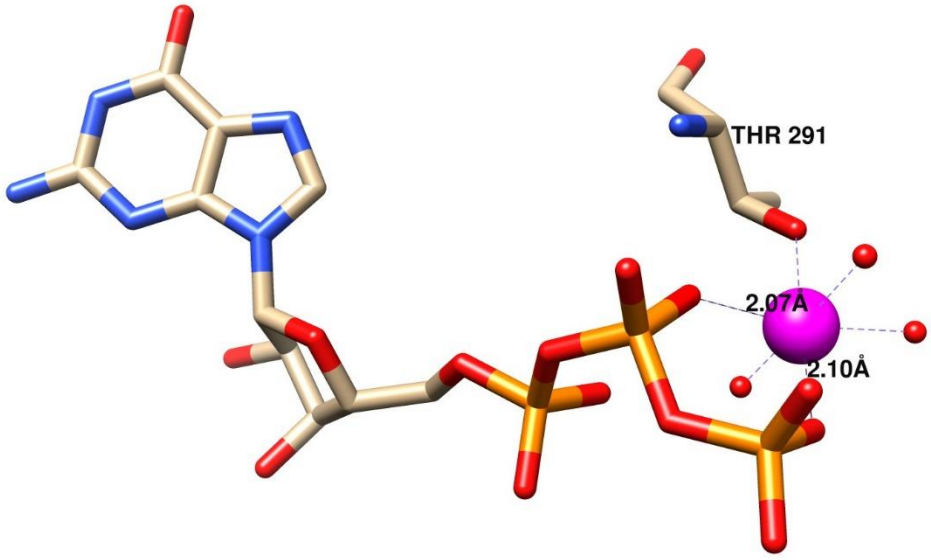

Figure 5.5: GTP in coordination with manganese M2 metal (pink) from PDB ID#2QEY. M2 cation is in octahedral coordination with T291 (P Loop) and cradling the β and γ phosphates.

5.4: The Omega Loop Closure

Once the Michaelis complex has been formed and all substrates are bound the final mobile element, the omega loop, must close over the active site. If one of the mobile loops, either P- or R-loop, is disordered it will sterically clash with the omega loop to prevent premature closure.[25] The P- and R-loop both have direct contacts with substrates, which lend energy to cause the mobile elements to adopt a closed formation.[24] The omega loop has to undergo a conformational change, but it does not directly interact with any substrates.[24] The energy required to cause this dynamic movement to a closed state is thought to come from the other substrates binding to the active site.[24] It is proposed that once OAA/PEP bind to the R-loop R87, enthalpic energy transfer is used to rotate the omega loop ~10 Å towards the active site.[24] R87 interacts with R89 to stabilize it into a conformation that allows H470 of the omega loop to bind, effectively "locking" the omega loop into a closed position.[25] Other neighbouring residues, S90, R483, E469 also stabilize the closed omega loop (Figure 5.6).[25] This closure shifts the P-loop, and therefore the nucleotide/metals (~1.5 Å) towards OAA to bring both substrates close enough together for in-line phosphoryl transfer (Figure 5.7).[25]

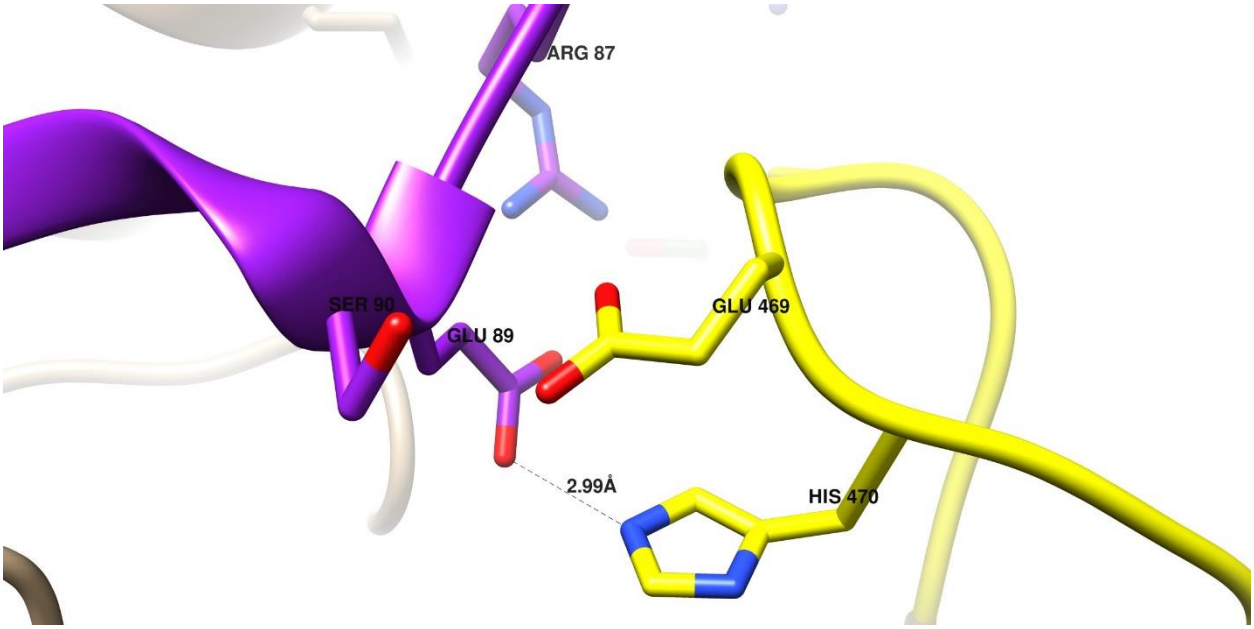

Figure 5.6: Omega loop (yellow) in closed order position contacting with R loop (purple) from PDB ID#2QF2.

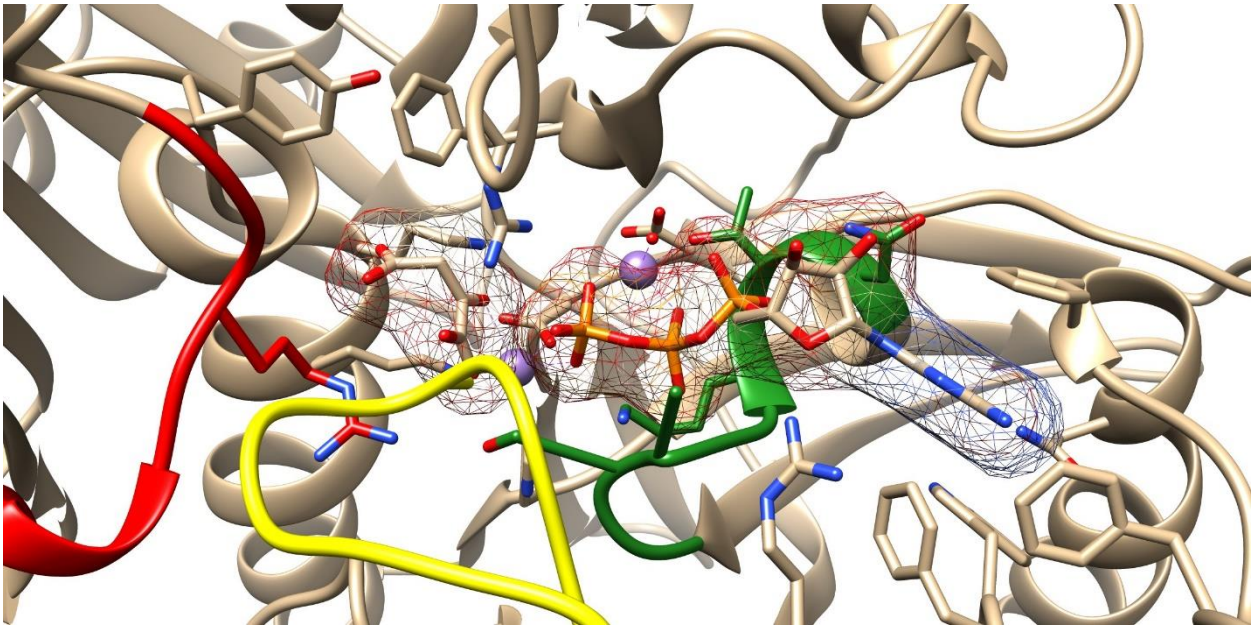

Figure 5.7: Michaelis complex with all mobile elements, R loop (red), omega loop (yellow), and P loop (green) in closed position. OAA is present in mesh on left, while GTP from PDB ID#2QEY in mesh is on right. Structure was generated from PDB ID#2QF2.

5.5: Catalysis

The first step of catalysis is the formation of the reactive enolate species.[9] This occurs through a decarboxylation of OAA, relinquishing CO_2. The CO_2 is stabilized by the rotation of Y235 (Figure 5.8).[9] Once the reactive enolate is formed, phosphoryl transfer occurs to create PEP.

5.6: Product Release

After catalysis, the energy donated from substrate binding has now been transferred. This changes the omega loop back to the open conformation.[9] PEP now shifts away from the M1 metal, while T235 rotates towards the interior of the enzyme, removing its interaction with CO_2 (Figure 5.9).[9] Now that PEP is not directly coordinated with the metal, PEP's P-loop interaction is also gone with S286.[9] This loss of interaction gives the P-loop the liberty to shift into its open state, moving the guanosine-3'-diphosphate and M2 away from M1.[9] With the omega loop and P-loop now in open states, both CO_2 and PEP are released.

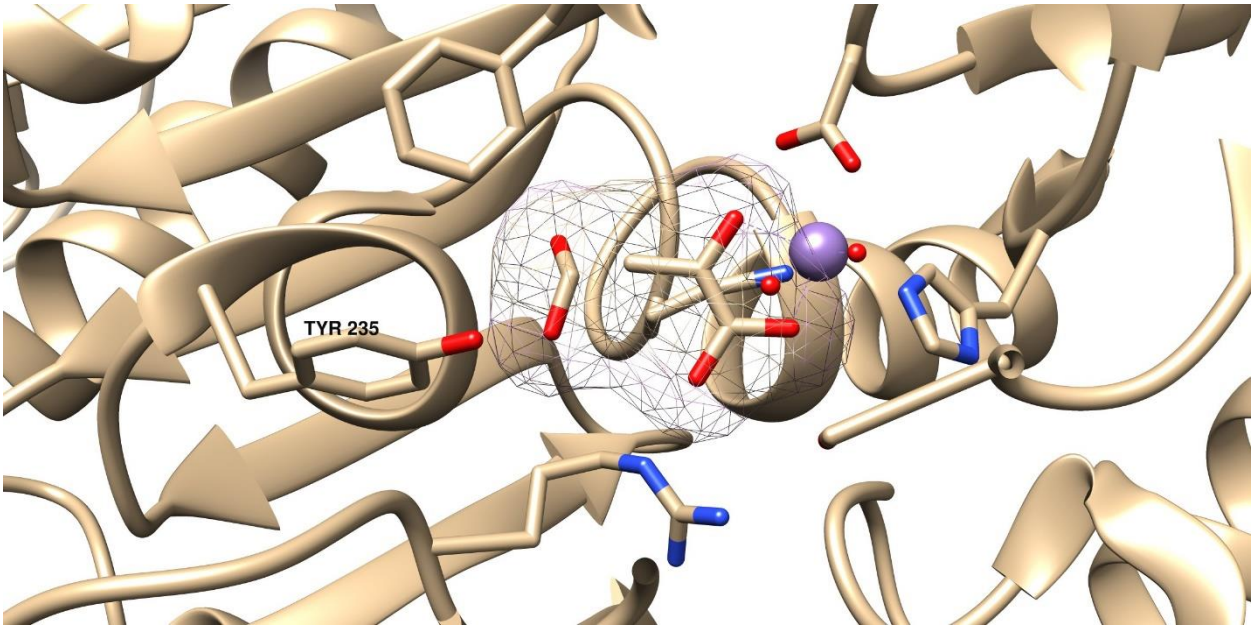

Figure 5.8: An alignment highlighting enolate intermediate coordinating with manganese M1 metal (purple) and CO_2 (modelled in mesh) from PDB ID#2QF2. Overall structure with Y235 in stabilizing conformation is from PDB ID#2RK8.

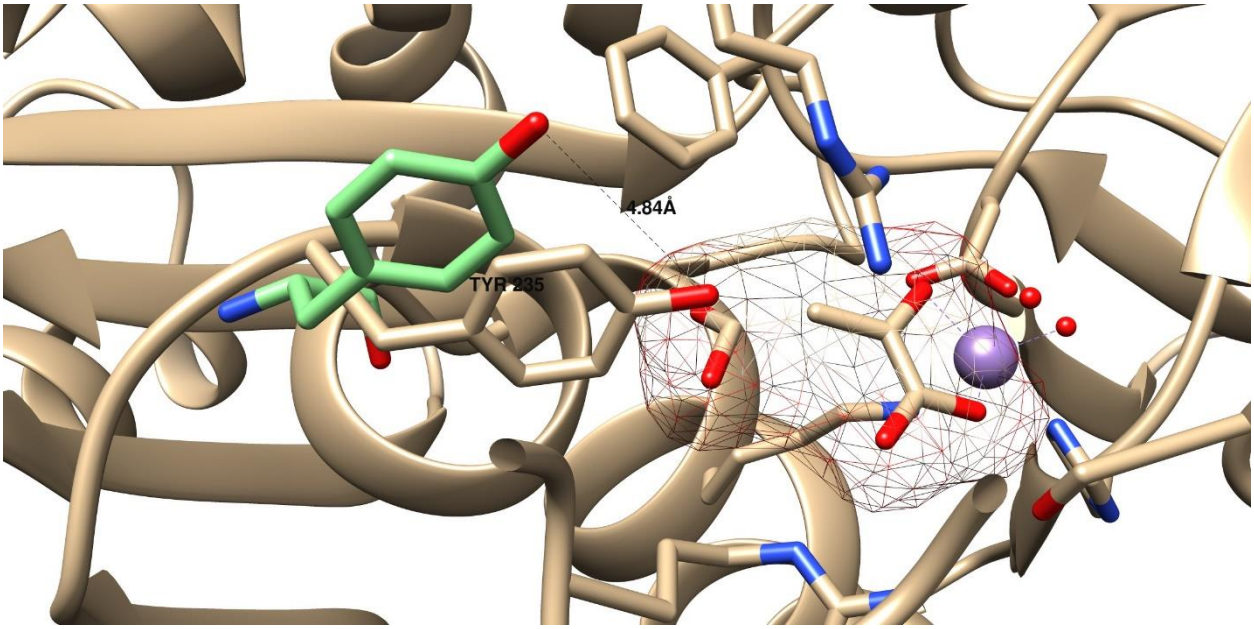

Figure 5.9: An alignment from PBD ID#2RK8 (tan) and PDB ID# 2QEW (light green) highlighting the two conformations of Y235.

Hypothesis

CMP will be utilized to study its potential as an inhibitor against three isozymes of PEPCK; *Mycobacterium tuberculosis,* rat cytosolic, and human mitochondrial. These three enzymes are all GTP-dependent enzymes with conserved active sites. It is expected that CMP will bind across the competitive OAA/PEP active site and adjacent secondary binding pocket in all three of the tested isozymes. Structural and kinetics characterization will be used to give insight into the degree and mechanism of inhibition of PEPCK by CMP.

Materials & Methods – Part 7: Protein Expression and Purification

7.1: Expression of Isozymes rcPEPCK & mtbPEPCK

Expression of rcPEPCK started with overnight cultures of BL21(DE3) E. coli with pET-SUMO vector containing the rcPCK gene. These cells were grown overnight at 37°C at 200rpm in LB media with kanamycin antibiotic at a concentration of 50µg/mL. The overnight culture was centrifuged for 10 minutes at 5000g. The resultant pellet was resuspended in fresh ZYP-5052 media. The resuspended pellet was transferred into four, 1L cultures of ZYP-5052 with 50µg/mL of kanamycin. The cultures were then incubated at 37°C at 200rpm for 16-20 hours. The cultures were then centrifuged at 7000g for 20 minutes, and the resultant pellets were frozen at -80°C.

7.2: Expression of hmPEPCK

The human mitochondrial isozyme (hmPEPCK) was expressed in BL21 (DE3) cells with pET-SUMO vector via IPTG induction. The four, 1L cultures were grown in LB media at 37°C until an OD_{600} of approximately 1.2. The temperature is then dropped to 20°C for 30 minutes. The cultures are induced with 0.1mM IPTG and express for 16-20 hours at 20°C. Cells are pelleted and frozen in the same manner as the rat cytosolic and *M. tuberculosis* expressions.

7.3: rcPEPCK Purification for Kinetics and Crystallography

All purification steps were completed at 4°C. The frozen pellets were extracted from their containers and resuspended in Buffer 1, refer to table 7.1, until a final volume of approximately 50mL. The homogenous solution was then loading to a prechilled French Press cell (4°C) and the cells were lysed at 20000 PSI twice. The lysed cells were then centrifuged at 12000g for 30-45 minutes to pellet the insoluble fraction. The supernatant was then removed and added to Qiagen Nickel-NTA resin pre-equilibrated in Buffer 1. The resin/supernatant combination was then mixed for 1 hour at 4°C. The resin was then washed with Buffer 1 until the flow through A_{280} was less than 0.1. Buffer 2 was the introduced to the resin to eluted the SUMO-fused protein. Fractions were collected and absorbance's were checked to determine which fractions held protein. These fractions were then concentrated with a 50mL Amicon Stirred Cell Nitrogen Spin Concentrator with a 30kDa Amicon HA-filter to a final volume of approximately 10mL. This protein solution was then incubated with SUMO-protease to liberate the SUMO-fusion tag overnight at 4°C. The resultant solution was buffer exchanged on a Bio-Rad P6DG polyacrylamide gel column which has Chelex-100 added to chelate contaminating metal ions, and pre-equilibrated in Buffer 3. The protein digest solution was added to the column, and fractions were taken. Fractions were checked spectrophotometrically again at 280nm, and fractions containing protein were concentrated to 10mL. This solution was then added to the Qiagen Nickel-NTA resin again that had been pre-equilibrated in Buffer 3. The protein/nickel was mixed for 1 hour to bind the SUMO-fusion tag. The solution was allowed to flow through and collected in fractions. The resin was then washed in Buffer 3 into fractions and all fractions containing protein were concentrated to 10mL. The now cleaved rcPEPCK was buffer

exchanged into buffer 4 via P6DG column pre-equilibrated in buffer 4. Fractions were collected of the protein sample now buffer exchanged in buffer 4, and they were concentrated down to a working concentration of 10-20mg/mL. The protein was then flash frozen in liquid Nitrogen in 20µL aliquots. The frozen protein was stored in a -80°C freezer. Purity was qualitatively assessed by SDS-PAGE.

7.4: mtbPEPCK Purification for Kinetics

The recombinant Mycobacterium tuberculosis PEPCK enzyme purification was the completed without deviation as stated above in the rcPEPCK. The differences between the two purification was that addition of 1mM EDTA and 0.1mM PMSF in the initial buffer 1. After the lysis and centrifugation to pellet the insoluble fraction, ammonium sulfate was added to the supernatant to a final saturation of 65%. The ammonium sulfate precipitation was stirred at 4°C overnight. The precipitation was then centrifuged at 12000g for 15 minutes. The pellet was resuspended in Buffer 1 without protease inhibitors (EDTA/PMSF).

7.5: hmPEPCK-SUMO Fusion Purification for Kinetics

The recombinant Human mitochondrial PEPCK purification was completed in the same manner as mtbPEPCK. The only deviation was the purification was completed after the initial Nickel-NTA and subsequent buffer exchange into Buffer 4. The enzyme was still fused to the SUMO-tag to help with solubility and stability.

Table 7.1: Purification Buffers for all kinetic protocols.

Buffer	HEPES (mM) pH 7.5	NaCl (mM)	Imidazole (mM)	Glycerol (%)	Reducing Agent
#1	25	300	10	10	2mM TCEP
#2	25	0	300	0	2mM TCEP
#3	25	0	0	0	2mM TCEP
#4	25	0	0	0	10mM DTT

All buffers were made a day prior to purification, and reducing agent was added immediately prior to starting.

7.6: hmPEPCK Purification – Cleaved

It has been a goal of mine of mine to optimize the purification protocol for the human mitochondrial PEPCK. This has been an effort in hopes for crystallographic structural work, increased yields and purity for biochemical analysis. In this new protocol, the purify is much higher then previous stated in section 1.5, but the yield is much lower. For basic kinetic analysis, the purification in section 1.5 is satisfactory, but a new protocol is necessary for different testing.

All purification steps were completed at 4°C. The frozen pellets were resuspended in buffer 5 and stirred to create a homogenous mixture. 0.1mM EDTA, 0.1mM PMSF, and finally 1mL of Calbiochem Protease Inhibitor Cocktail 7 was added to prevent proteolysis during the initial stages of purifications. The solution was then loaded into a prechilled French press cell (4°C) and the cells were lysed at 20000PSI, twice. The lysis was then centrifuged for 30minutes at 12000g. The supernatant was removed from the insoluble pellet and ammonium sulfate was

added to a final concentration of 65%. The ammonium sulfate precipitation was incubated overnight at 4°C. The ammonium sulfate precipitation was centrifuged at 12000g for 15 minutes. The supernatant was removed and the pellet was resuspended in buffer 1 without EDTA, PMSF, or Cocktail 7. The solution was added to pre-equilibrated Nickel-NTA resin from Qiagen, and the protein solution/Nickel-NTA was incubated for 1 hr at 4°C. The resin was washed with buffer 1 until the flow through A_{280} was below 0.1, at this point buffer 6 was used to elute the SUMO-fused hmPEPCK from the nickel resin. Fractions were collected, and fractions containing protein were concentrated with a 30kDa cutoff Amicon HA-filter to approximately 10mL. The resultant solution was buffer exchanged on a Bio-Rad P6DG polyacrylamide gel column which was chelexed and pre-equilibrated in Buffer 7. Fractions were collected and enzyme containing fractions were concentrated to approximately 4-5mL. The enzyme containing solution was added to Ceramic Hydroxyapatite type 2, 20µm resin via a FPLC. The protein was then eluted with a gradient of 5-400mM KPO_4^- (buffer 7-8). Fractions are checked for SUMO-fused hmPEPCK via SDS-PAGE, and concentrated to 10mL. A second buffer exchange into buffer 8 via P6DG desalting column and concentrated again to 10mL. One aliquot of SUMO-protease is added to the solution and left overnight at 4°C to remove the SUMO-tag. Flocculation is seen, with major loss of PEPCK precipitation. The resultant soluble cleaved enzyme is incubated for 1 hour at 4°C with pre-equilibrated Nickel-NTA resin. Flow-through is collected, and the resin is washed with buffer 7. All fractions with A_{280} above 0.1 were concentrated to 10mL. The solution was then buffer exchanged a final time into buffer 9. The buffer exchanged protein solution was concentrated to a stock concentration of 10mg/mL,

and flash-frozen in liquid nitrogen in 20µL aliquots. Final purity was checked via SDS-PAGE (Figure 10.1).

Table 7.2: Purification buffers for hmPEPCK purification to get a highly purified monospecies.

Buffer	KPO_4^- (mM) pH 6.8	NaCl (mM)	Imidazole (mM)	Glycerol (%)	Reducing Agent
#5	5	300	10	10	2mM TCEP
#6	5	0	300	0	2mM TCEP
#7	5	0	0	0	2mM TCEP
#8	400	0	0	0	2mM TCEP
#9	5	0	0	0	10mM DTT

Materials and Methods - Part 8: Kinetic Assays

8.1: PEP → OAA – Dephosphorylation and Carboxylation

The enzymatic activity and inhibition assays were determined by evaluating various concentrations of inhibitor as well as substrate. The reaction was measured at 340nm in a Cary 100 UV spectrophotometer by the oxidation of NADH at 25°C. The corresponding kinetic values were calculated based off of data obtained in the anaplerotic reaction, the conversion of phosphoenolpyruvate to oxaloacetic acid. The reaction mixture contained 50mM HEPES pH 7.5, 10mM DTT, 100µM $MnCl_2$, 4mM $MgCl_2$, 1mM GDP, 300µM NADH, 50mM $KHCO_3^-$, 10 units of MDH, and 2.5µg of PEPCK, with varying concentrations of PEP from 10-4000µM. The reaction was measured with the addition of both PEPCK and MDH simultaneously. The reaction mixtures were incubated at 25°C for a minimum of 5 minutes to ensure steady temperature. Human mitochondrial PEPCK was incubated with 5% Chelex 100 for 1 hour, followed by subsequent centrifuge and filtering. 100mM $KHCO_3^-$ was also used for all assays against human mitochondrial PEPCK.

8.2: IC_{50} Determination

The IC_{50} values were determined by evaluating enzyme activity with fixed substrate concentration, and varying inhibitor concentration. The assay mixture was fixed at 500uM PEP, and all other assay conditions are same as section 8.1. GraphPad Prism 8 software was used to

create plots and calculated IC_{50}. From IC_{50}, K_i were determined from the Database Resource for Clostridial Neurotoxins algorithm, fitting to the equation 12.3.

8.3: Data Analysis

All data analysis was completed with SigmaPlot11 with the Enzyme Kinetic module. All of the data were fit to equation 1, and respective K_m and V_{max} values were used to create replots of K_m/V_{max} and $1/V_{max}$ to determine the K_i values of CMP against the various isozymes studied.

Materials and Methods – Part 9: Structural Studies

9.1: Crystallization of rcPEPCK

Co-crystallization of CMP with rcPEPCK was completed by setting hanging drops of mother liquor containing 0.1M HEPES pH 7.5, 24-34% PEG 3350, 0.5µL of 5mM CMP, and 0.5µL of 10mM $MnCl_2$, and varying amounts of rcPEPCK (~10mg/mL). Various drops size/ratios were used from 2:2, 2:4, and 4:2 (protein to mother liquor in uL) were equilibrated over 1-3 days until crystals were formed. Crystals were harvested and cryoprotected in 0.1M HEPES pH 7.5, 35% PEG 3350, 10%PEG 400, 2mM $MnCl_2$, and 1mM CMP. These cryoprotected crystals were then flash frozen in liquid nitrogen for long term storage.

9.2: Data Collection

Cryocooled crystals were sent to the CMCF Beamline 08ID-1 at the Canadian Light Source in Saskatoon, Saskatchewan. Data was indexed, scaled, and integrated using HKL2000.

9.3: Determination and Refinement

rcPEPCK_CMP was solved with molecular replacement using MOLREP in CCP4 with the previously solved structure of PEPCK_Mn^{2+} PDB ID#2QEW. The structure was refined with Refmac5 and manual building in COOT. Water validation was completed through COOT.

Results - Part 10.1: Kinetic Analysis of CMP

Kinetic characterization were all completed using the assays outlined in section 8.1. The results are tabulated in Table 10.1, and the K_i values presented are taken from the K_m/V_{max} vs [I] replot. The K_i values determined were 29+/-2.8uM, 54.8+/-3.0uM, and 83.4+/-8.0uM for the rat cytosolic, *Mycobacterium tuberculosis*, and human mitochondrial PEPCK respectively.

Table 10.1: Kinetic Characterizations of CMP and PEPCK

Enzyme	K_i from Replots (uM)	K_i From Fits (uM)	Mode of Inhibition
Rat Cytosolic	29.0+/-2.8	11.8+/-1.4	Competitive
Mycobacterium Tuberculosis PEPCK	54.8+/-3.0	45.7+/-3.5	Competitive
Human Mitochondrial	83.4+/-8.0	46.0+/-9.3	Competitive

IC_{50} characterizations were completed using assay outlined in section 8.2. The results are tabulated below in Table 10.2. Each of the IC_{50} values were taken and an expected K_i was determined. These K_i values are 3.8+/-0.5uM for human mitochondrial PEPCK vs 3-MPA, 57.9+/-7.2uM for human mitochondrial vs CMP, and finally 35.9+/-9.7uM for Rat cytosolic vs CMP. Full curves can be seen in the appendix.

Table 10.2: IC_{50} Characterizations

Enzyme & Inhibitor	IC_{50} (uM)	Calculated K_i	Goodness of Fit R^2
3-MPA vs Human Mitochondrial	7.5+/-0.6	3.8+/-0.5	0.99
CMP vs Human Mitochondrial	115.7+/-9.6	57.9+/-7.2	0.99
CMP vs Rat Cytosolic	107.8+/-27.2	35.9+/-9.7	0.97

10.2: Purification of hmPEPCK

The complete purification protocol for human mitochondrial PEPCK optimized to create a monospecies for further structural studies. Figure 10.1 below shows SDS-PAGE at various steps of the purification protocol.

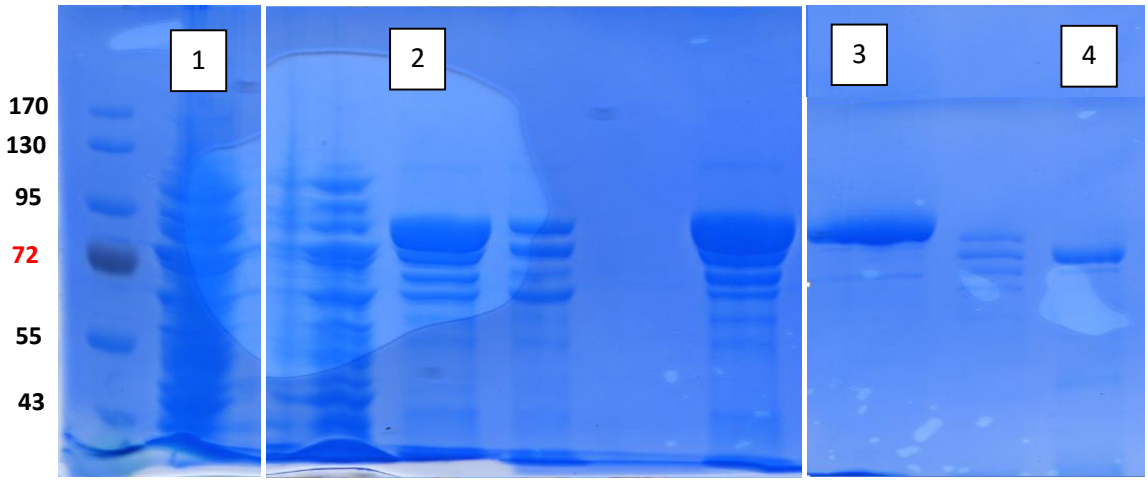

Figure 10.1: SDS-PAGE to check the purity of the human mitochondrial PEPCK. Lane 1 is lysate, lane 2 is after nickel chromatography, lane 3 is after CHT chromatography, and finally lane 4 is after SUMO digest and second nickel chromatography.

After SUMO digestion, and binding to the nickel-NTA resin, there is major precipitation of protein. As seen from lanes 3 and 4, there is a high level of purity that can be obtained.

10.3: Structural Determination of rcPEPCK-CMP

The cocrystallized structure of rcPEPCK and CMP was determined, with all data statistics present in the appendix. There is excellent electron density in part due to the high-resolution of the data (1.5Å), and therefore CMP was modelled very easily. In summary, the space group is $P2_1$, with resolution limits of 59.4-1.49Å and redundancy of 4.8. A complete dataset was collected of 360° in 1° increments.

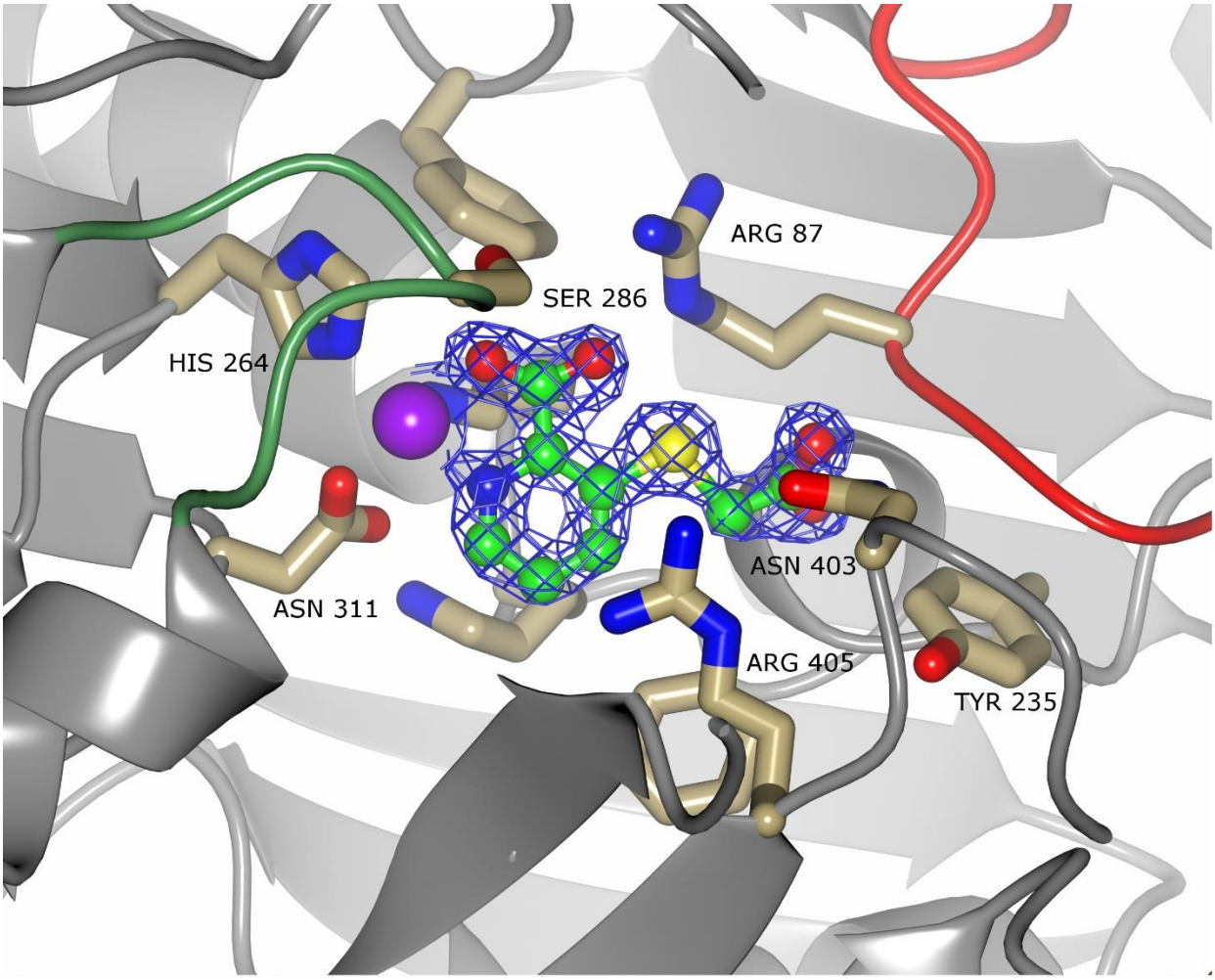

Figure 10.2: CMP bound to active site manganese M1 metal (purple). The P-loop and R-Loop are both coloured in green and red respectively, while atoms are coloured by type. All binding residues are also highlighted. CMP is modeled into the experimental electron density (blue, 2Fo-Fc, rendered at 1.5 sigma). The resolution of structure is 1.5Å. Image was rendered in CCP4MG.

Discussion – Part 11: Inhibition of PEPCK by CMP

11.1: 3-Mercaptopicolinic acid and Its History of Inhibition

PEPCK's role in metabolic homeostasis, and its new emphasis in various clinical maladies makes the enzyme a very attractive therapeutic target. By specifically targeting PEPCK, conclusions can be drawn with regards to its specific role. Crystal structures of the various PEPCKs have only been available in the last 20 years but many studies determining inhibitors of gluconeogenesis, and specifically PEPCK, have been completed since the 60's. A combination of both structural work, and inhibition studies are now finally starting to elucidate molecular scaffolds that can be used to build more potent and selective inhibitors. Of these initial inhibitors studies, tryptophan and its metabolites were determined to have an effect on PEPCK turnover.[45,50,64] Saunders *et al* determined that 3-mercaptopicolinic acid was a novel inhibitor of gluconeogenesis.[8] A year later, non-competitive inhibition of PEPCK with 3-mercaptopicolinic acid was seen in both mitochondrial and cytosolic fractions, with the cytosolic enzyme being more potently inhibited.[47] With the confirmation that 3-mercaptopiconlinic acid inhibits PEPCK, a mechanism of action had to be determined. Baum, Schramm, and Hanson in 1975 proposed a mechanism for the non-competitive inhibition pattern. They proposed that 3-mercaptopicolinic acid was acting by chelating the M1 manganese ion from the active site of the enzyme.[26] In contrast to the chelation theory, Nowak and Makinen suggested that 3-mercaptopicolinic acid may bind in an overlapping binding site, resulting in an unfavourable conformation change.[35] This accounts for the K_m and V_{max} effects seen in their inhibition studies, but they could not rule out the idea that 3-mercaptopicolinic

acid also bound to a secondary allosteric site.[35] With an unconfirmed mechanism, crystallographic data was required to fully explain this mixed inhibition. Holyoak and his colleagues published this structural and kinetic work determining that 3-mercaptopicolinic acid actual bound in two different sites, at the active site and a second behind the P-loop of PEPCK, Figure 11.1.[2]

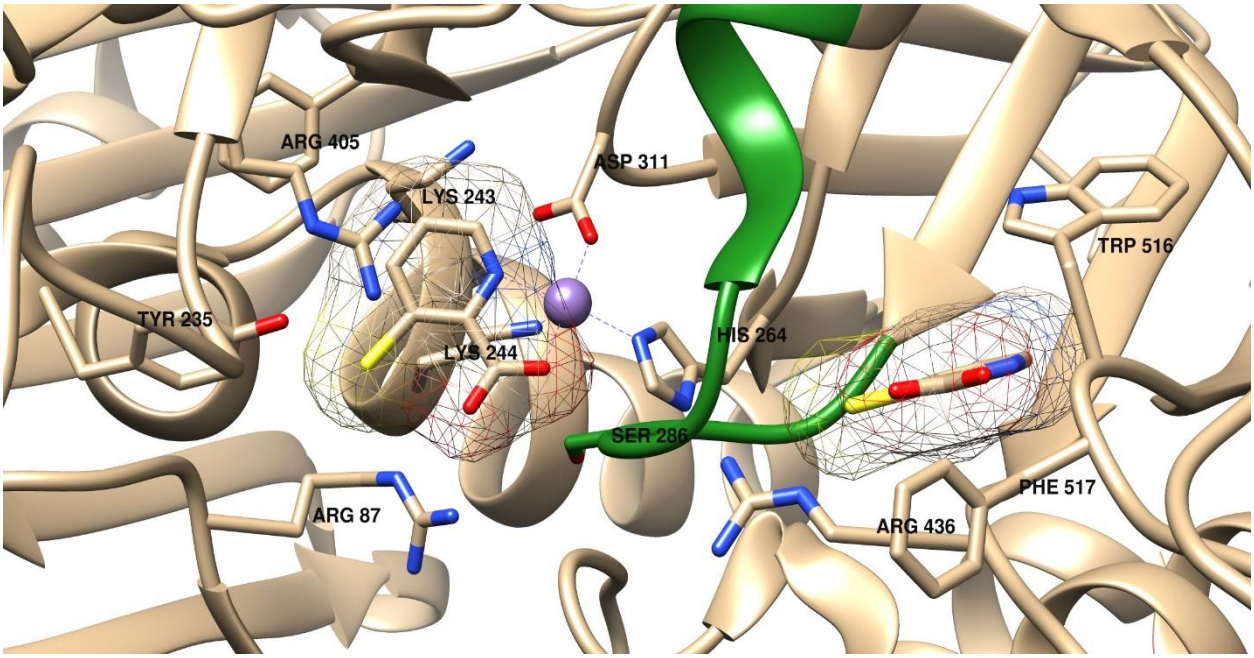

Figure 11.1: 3-MPA bound to both the active site in a competitive fashion (left), and the secondary allosteric binding pocket (right) generated from PDB ID#4YW8. The P-loop is highlighted in green, while the 3-MPA molecules are covered in mesh.

11.2: Further Inhibitory Studies and Adjacent Binding Cleft

The need for more selective inhibitors would allow for targeted inhibition of PEPCK, resulting in an elevated understanding of metabolism, various biomedical maladies, and enzymology. In 2008, the Holyoak lab conducted various screens against rat cytosolic PEPCK and prospected inhibitors.[54] Of these inhibitors, a few had very low K_i values and one in particular had an interesting mechanism of inhibition. The inhibitor, sulfoacetate, is of particular interest to the work within this body. Through crystallographic data, sulfoacetate was shown to bind in a neighbouring adjacent pocket to the PEPCK active site M1 metal with a K_i of approximately 85uM.[54] This new pocket opens only with the movement of Y235 away from the active site, and towards the interior of the PEPCK. This rotation is seen after OAA has been decarboxylated and has been phosphorylated to form PEP. Sulfoacetate forms an edge on interaction with Y235, stabilizing them into the new cleft (Figure 11.2).[54]

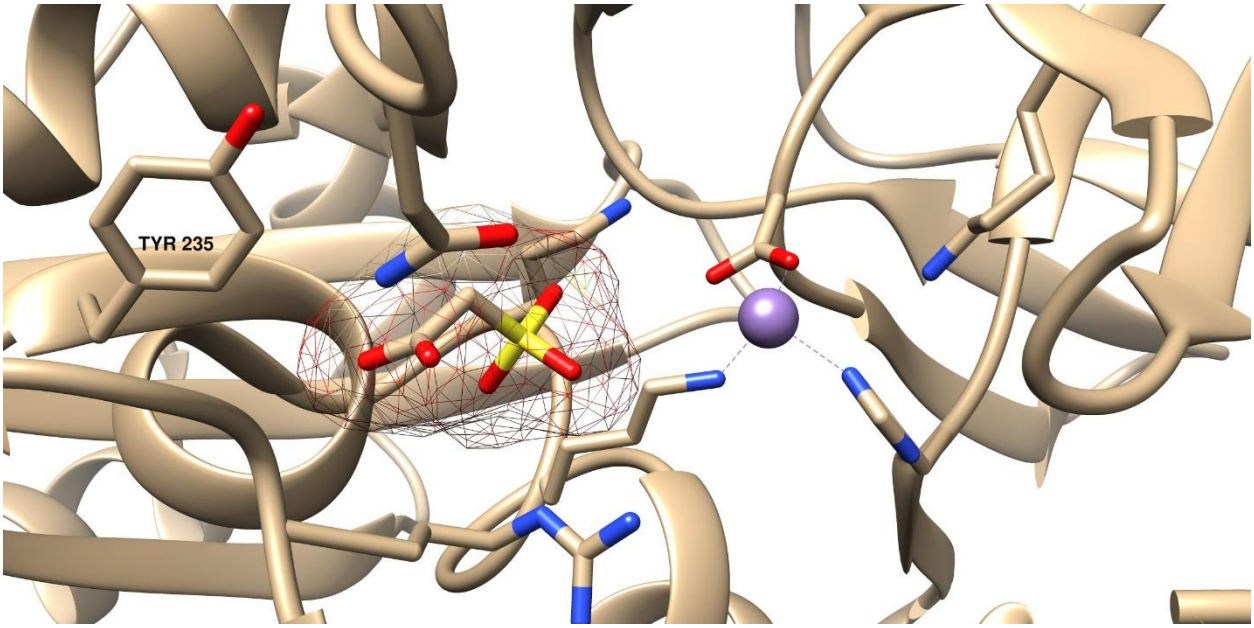

Figure 11.2: Mechanism of inhibition of sulfoacetate from PDB ID#2RKE. Please note Y235 is rotated into the PEP-bound orientation and sulfoacetate is highlighted in mesh.

11.3: Inhibition of PEPCK: Conception of Carboxymethyl-thiol-picolinic Acid

Based on the 3-mercaptopicolinic acid work and the sulfoacetate inhibition mechanism, the question arises if both the active site competitive inhibition mechanism can be exploited in conjunction with this new adjacent binding pocket.[55] From the scaffold of 3-mercaptopicolinic acid a new molecule was created, carboxymethyl-thio-picolinic acid (CMP). By extending the sulfhydryl tail of 3-mercaptopicolinic acid with a carboxyl group, the aim is to have an increase selective inhibition of PEPCK. Figure 12 indicates superimposed images of 3-mercaptopicolinic acid inhibition with sulfoacetate. As can be seen, the overlapping sulfur atoms of both groups allow for a possible bridge between the two inhibitors.

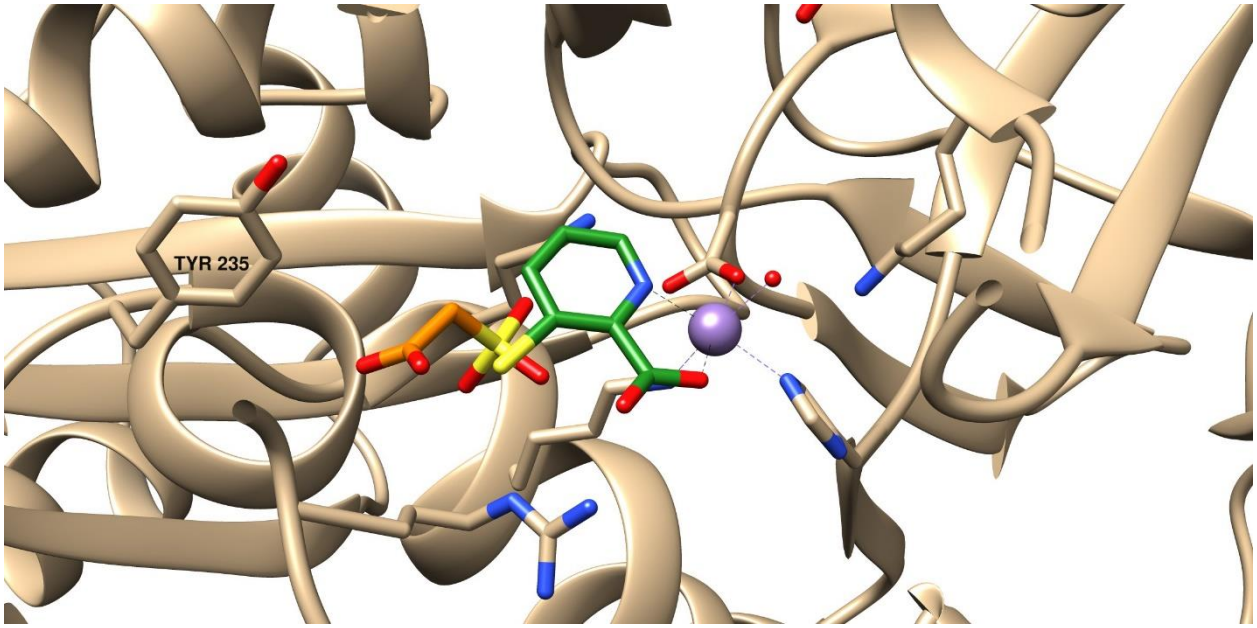

Figure 11.3: Superimposion of PBD ID# 4YW8 and 2RKE. 3-mercaptopicolinic acid is the molecule in green, while sulfoacetate is in orange. Also note, that Y235 is in the PEP-bound orientation, allowing for sulfoacetate to bind.

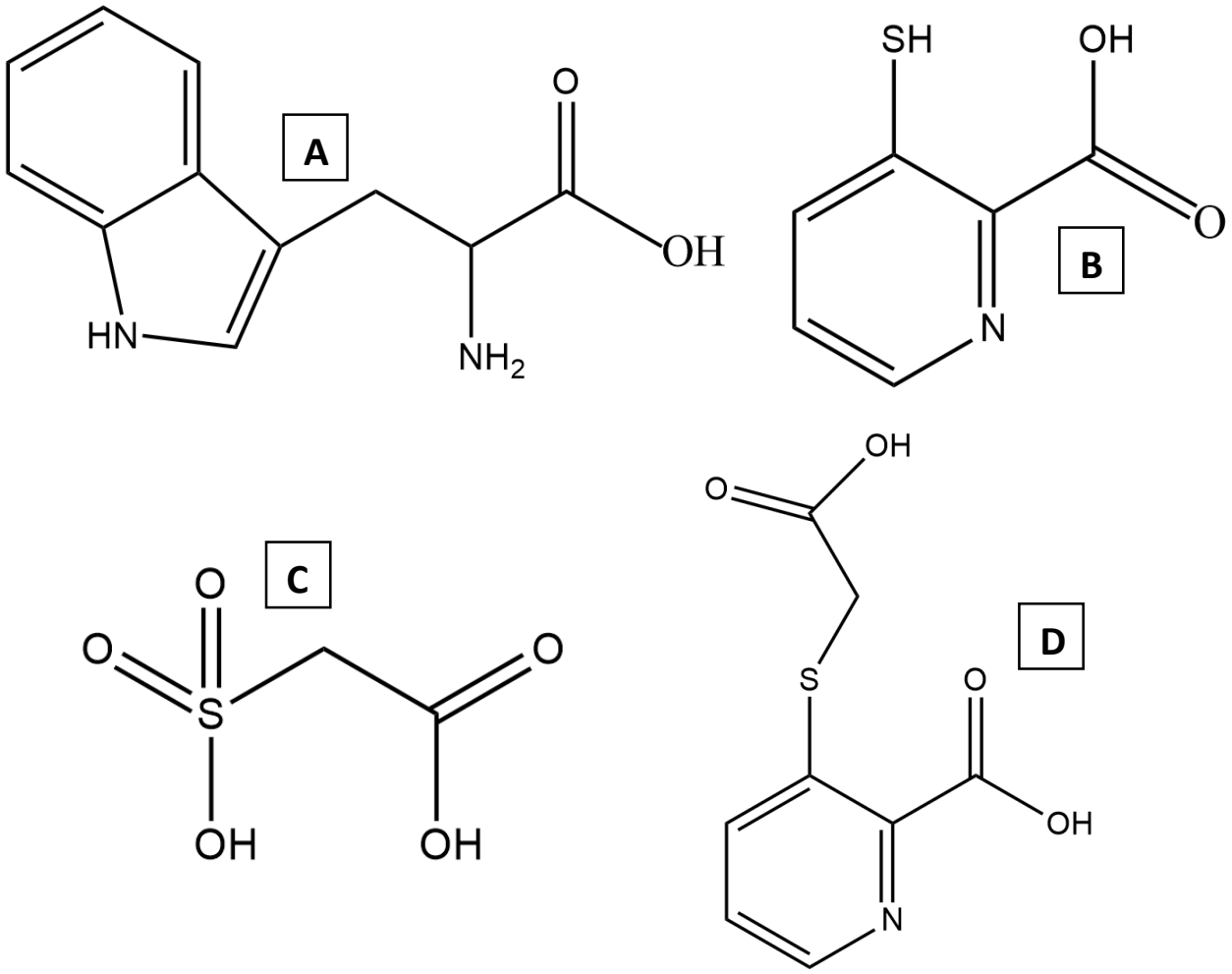

Figure 11.4: Molecular structures of potential inhibitors of PEPCK. A, tryptophan, B, 3-mercaptopicolinic acid, C, sulfoacetate, and D, carboxymethyl-thiol-picolinic acid.

11.4: Inhibition of PEPCK by CMP

The focus of this project was to create a more selective inhibitor for PEPCK, by simultaneously occupying the OAA/PEP active site, as well as an adjacent secondary sulfoacetate binding pocket (Figure 11.2). The addition of the carboxymethyl tail onto the sulfhydryl of 3-MPA would potentially create a molecule that could inhibit PEPCK through this new mechanism. The structural insight from the cocrystallization of CMP to the rat cytosolic PEPCK shows that CMP does bind to PEPCK, concurrently occupying the OAA/PEP and the adjacent site as predicted. This inhibition mechanism is proposed to occur in all PEPCK because of the enzymes highly conserved active site. Seen in figure 11.5, CMP binds in coordination with the M1 manganese metal in the same position as 3-MPA with the nitrogen and carboxyl of picolinic acid, while CMPs carboxy tail extends into the PEP binding region. This is the same position and mechanism that was hypothesized for CMP.

Figure 11.6 shows the various residues of the active site and their interaction with CMP. All binding residues are conserved from 3-MPA and CMP. Because of the extension of the carboxy tail, an additional residue A403 can now interact with CMP. When PEP is bound to the active site, A403 amide and backbone nitrogen interacts with O2 at distance of 2.9 Å through H-bonding.[25] As seen in figure 11.6, this binding pattern is conserved. Structural overlaps (data not shown) between rcPEPCK-CMP and PEP bound PEPCK (PDB ID# 4GMW), show the orientation of A403 and Y235 are completely conserved.

The addition of the carboxy tail moiety also removes the allosteric effect that 3-MPA exhibited against rat cytosolic PEPCK. The size and length of CMP would prevent it from binding behind

the P-Loop, and the added protection of the reactive thiol by the carboxy tail extension prevents covalent disulfide binding to C288 shown when MPA bind in the allosteric pocket.[2]

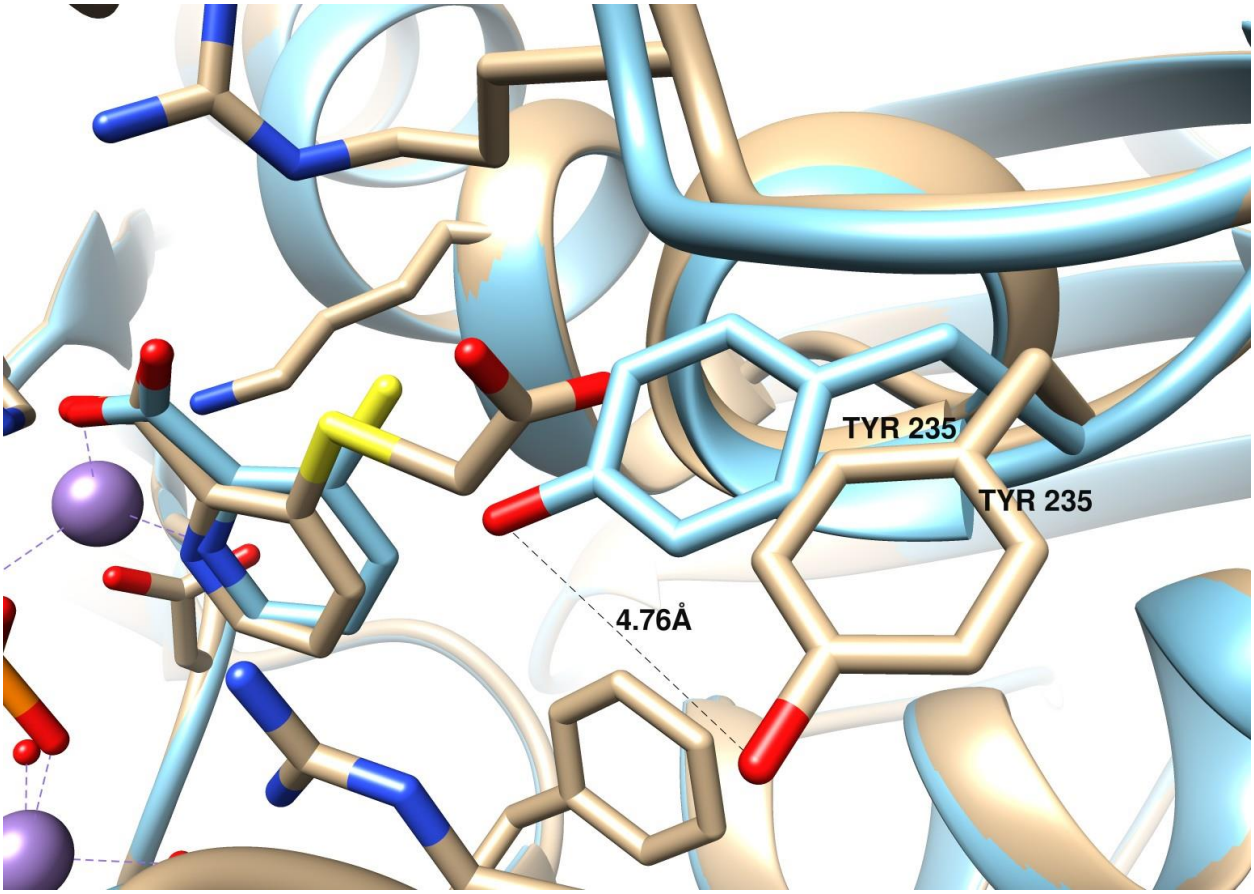

Figure 11.5: Structural overlap of rcPEPCK-CMP (tan) and PDB ID#4YW9 (light blue). CMP is shown to overlap with 3-MPA at the active site. The rotation of Y235 from the open position to the closed position. The hydroxyl of tyrosine appears to move ~4.8 Å to make space for the carboxy tail moiety of CMP.

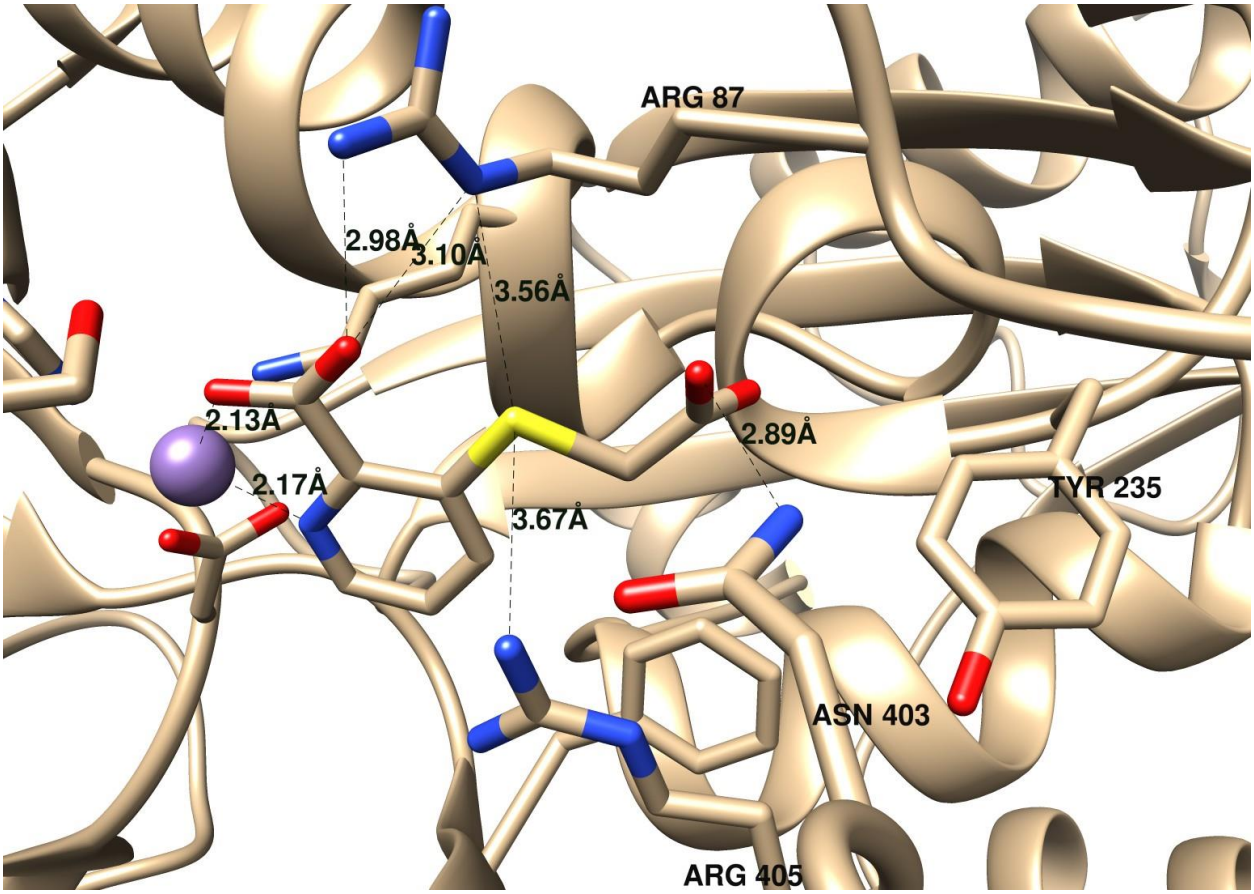

Figure 11.6: rcPEPCK-CMP with all binding residues that interact with CMP. E403 appears to interact with a carboxyl oxygen of the carboxy tail as proximity is measured to ~2.9 Å*.*

With the exact position and mechanism of CMP's inhibition determined through the structural work, the potency of the interaction was determined through inhibition assays. CMP was assayed against the various isozymes of PEPCK to determine an experimental K_i value. This K_i will represent the potency of inhibition and further explain the inhibition pattern seen in the structural work. The K_i values listed in table 10.1 were all taken from K/V vs [I] replots, as well as from the full set of curves fitted to a competitive model. The 1/V vs [I] replot (see appendix) for all of the inhibition assays show that there is a small intercept effect present, as the V_{max} decreases slightly. This can be attributed to a partial chelation effect of CMP for M1 metal ions. This would effectively reduce the overall amount of competent enzyme able to bind and catalyse substrate, decreasing the V_{max}. This behaviour is also seen with 3-MPA and other picolinic acid derivatives.[2] This chelation effect changes the inhibition model from a competitive one as seen from the structural work, to a mixed inhibition model. The inherent problem with using a mixed inhibition model for documenting inhibition constants is at low concentrations of CMP, there is very little attributable chelation, but at high concentrations this effect is more drastic. This interesting mode of inhibition will cause inaccuracies in fitted data, whereas the replot may more accurately reflect the inhibition constants. For this reason, in conjunction with the structural data presented a competitive inhibition model was used for the global fits. Lastly, the K_i values from the K/V vs [I] replots were used for analysis and discussion of the inhibition potency.

Based on the conservation of PEPCK's active site, the overall inhibition mechanism and potency should be comparable across each of the isozymes tested with only minor variations because of specific enzyme dynamics. With conservation of the active sites and the minor differences in

potency, there should be an inability to selectively inhibit one isozyme of PEPCK while leaving the others unaffected. When examining the relative inhibition of CMP to each of the isozymes, they are all selectively inhibited based on structural work and active site conservation but there is a small decrease in potency (30uM, 50uM to potentially 83uM for rat cytosolic, *Mycobacterium tuberculosis* and human mitochondrial PEPCK respectively). Although not greatly significant, it is interesting nonetheless that there is 2-3 fold difference in inhibition between rat cytosolic and human mitochondrial PEPCK. To better understand this slight difference in potency structural work on the human mitochondrial isozyme will have to be completed, so the conformational dynamics of the enzyme can be understood.

Under the assumption that the Ki values documented in table 10.1 are accurate representations of the binding constants of CMP, conclusions can be drawn with regards to the conformational dynamics of each isozyme. Although the active sites are conserved, the rest of the enzyme is variable. These structural variations are necessary for the enzyme to adopt differing conformations, some that are productive while others are not.[58] Enzymes are dynamic systems that will sample all conformations at varying rate. This differing sampling rate between productive and non productive conformers between isozymes will create different population distributions.[58] These average population distributions influence the rate of substrate binding of the enzyme, which will influence kinetic binding constants.[58] The omega-loop is one influence in the differential conformational population distributions as it must be open to allow for substrate binding. Once PEPCK has encountered substrates in a productive conformation, many dynamic transitions from unordered to ordered state must occur for the enzyme to commit to catalysis.[58] The motion of the omega-loop to a closed state after substrate binding is

required for catalysis to occur.[25,58] Upon closure of the omega-loop the dielectric constant of the active site will decrease as water is removed, harbouring tighter binding of the substrates/inhibitors to the enthalpic residues through increased electrostatic interactions.[25] If the omega-loop across the isozymes transition from open to closed states at differing rates between isozymes, the binding constants will vary. Sullivan and Holyoak in 2008 showed that even during the Michaelis complex, there is a propensity for the omega-loop to occupy an open state (~20%).[58] The omega-loop shows that isozymes having dynamic variation in both: population shifts of productive and non-productive conformers that allow for substrate binding, as well as rate of conformation shifts to catalytically competent conformers to orient substrates to commit to catalysis. PEPCK's system of conformational dynamic is still more complex, but this example reinforces the idea that isozymes can have different kinetic parameters even with all catalytic binding residues being conserved. This could be an explanation for the different K_i observed between the isozymes tested and CMP.

Unfortunately, the K_i value (83uM) documented for human mitochondrial PEPCK is only an approximation as a full inhibition curve could not be completed. There was not enough CMP available to complete the higher concentration points for CMP. More CMP will be synthesized in the future to complete the inhibition data.

In light of this approximation, IC_{50}'s and the corresponding K_i were determined for human mitochondrial PEPCK. The K_i determined is approximately 58uM and the accuracy of my IC_{50} determination was validated by testing the IC_{50} for CMP against rat cytosolic PEPCK. The K_i of CMP for rat cytosolic PEPCK from IC_{50} determination (36uM) was quite similar to that

determined through complete kinetic analysis (30uM), showing strong correlation of IC_{50} determined K_i and the inhibitory constants found from complete inhibition curves.

When comparing the inhibitory effect of CMP and 3-MPA, 3-MPA was shown to have a K_i of approximately 10uM against the rat cytosolic PEPCK (competitive site). In contrast, CMP has a K_i of 30uM. This small decrease in inhibition may be caused by the free energy landscape changing. Both enthalpic and entropic contributions effect binding affinities of small ligands to proteins through Gibbs' free energy. Based on the structural information for rcPEPCK-CMP, the overall enthalpic contributions should increase as now an additional residue, A403, will interact with CMP. To offset this new enthalpic energy that is gained, the entropic penalty of the carboxy tail will lower the free energy of the system. Due to the decrease in binding affinity, the entropic penalty must be greater than the enthalplic energy contribution. There is no information on the inhibitory constant of 3-MPA and the *Mycobacterium tuberculosis* PEPCK, but due to the conserved active site, it is probably similar to the K_i of 3-MPA and rat cytosolic PEPCK.

Last, because of expected K_i of CMP for human mitochondrial PEPCK is potentially 2-3 times higher than the other two isozymes tested, the binding affinity for 3-MPA for this isozyme was also determined. This was investigated to see if there was an inherent difference in the inhibition of human mitochondrial PEPCK for 3-MPA and other picolinic acid derivatives. This inherent difference could manifest itself through varying K_i value. Once calculated the K_i was determined to be 3-4uM, showing tighter binding of 3-MPA by 2 fold more than the rat cytosolic inhibition. This tighter binding of 3-MPA for human mitochondrial PEPCK may be an artifact of 3-MPA binding to both the competitive site and the allosteric site. These two

binding locations for 3-MPA could compound to cause a greater inhibitory effect and decrease in K_i. These similar K_i documented for CMP may have a lower binding affinity for human mitochondrial PEPCK because a slower conformational shift to a state readily available for inhibition by CMP. The dynamic difference causing a change in K_i could be in the PEP binding pocket, and in relation to Y235. This difference would not manifest itself in inhibition of PEPCK by 3-MPA, but would with the mechanism of CMP. Structural information on human mitochondrial PEPCK is required to validate this hypothesis.

In closing, the structural and kinetic work clearly shows the new inhibition mechanism of CMP. CMP binds by bridging the OAA/PEP binding site and the adjacent secondary CO_2 binding site, and this mechanism should be preserved in all PEPCK isozymes based on active site conservation. The potency of CMP shows variation across isozymes tested, with the greatest difference of 2-3 fold between rat cytosolic (K_i ~30uM) and human mitochondrial (K_i ~83uM). Although not greatly significant, this may indicate dynamic conformational differences between these two isozymes.

Conclusion and Future Directions:

The need for highly selective inhibitors of PEPCK is apparent, as PEPCKs inhibition could be used to further our understanding metabolism as a whole and the various maladies PEPCK has been implicated in. From initial inhibition studies tryptophan metabolites, and more specifically 3-mercaptopicolinic acid, showed potent inhibition of all PEPCK isozymes based on the conservation in the active site. Based on structural and inhibition studies, carboxymethyl-thiol-picolinic acid was designed to improve the scaffold of 3-MPA to create a more selective, and hopefully potent, inhibitor of PEPCK that can bind both the OAA/PEP active site as well as a secondary adjacent binding site simultaneously. The work presented here shows a slight decrease in potency (10uM and 30uM K_i inhibition for 3-MPA and CMP respectively), but hopefully increases selectivity as a secondary adjacent binding site is now utilized by CMP.

With the new crystallographic structures of PEPCK, the active site architecture can be exploited when creating new inhibitors for PEPCK. Although 3-mercaptopicolinic acid has been shown to be a more potent inhibitor, CMP should in theory be a more selective inhibitor as it now utilizes a secondary binding pocket. From the new scaffold of CMP, modifications could be introduced to extend the molecule into other areas of the active site. Although this work has shown the potency and mechanism of action, *in vivo* studies are necessary to determine the efficacy of the inhibitor. This inhibitor could be used against various cancer cell lines, *Mycobacterium tuberculosis*, as well as human mammalian cells. Based on the structural conservation of the PEPCK active site, there should not be a great difference in potency across PEPCK isozymes, but its selectivity for PEPCK could be tested.

There has also been a call within literature for a greater understanding of the human mitochondrial PEPCK, as its function and purpose has still not fully been defined. This work contributes to this as it identifies a potential difference in inhibition potency between the cytosolic and mitochondrial PEPCK. Structural insight would be a great help in elucidating the questions surrounding human mitochondrial PEPCK.

References:

1. Akram, M. Citric Acid Cycle and Role of its Intermediates in Metabolism. *Cell Biochem. Biophys.* **68,** 475–478 (2014).

2. Balan, M. D., McLeod, M. J., Lotosky, W. R., Ghaly, M. & Holyoak, T. Inhibition and Allosteric Regulation of Monomeric Phosphoenolpyruvate Carboxykinase by 3-Mercaptopicolinic Acid. *Biochemistry* **54,** 5878–5887 (2015).

3. Ballard, F. J. & Hanson, R. W. Phosphoenolpyruvate carboxykinase and pyruvate carboxylase in developing rat liver. *Biochem. J.* **104,** 866–871 (1967).

4. Ballard, F. J. & Hopgood, M. F. Phosphopyruvate carboxylase induction by L-tryptophan. Effects on synthesis and degradation of the enzyme. *Biochem. J.* **136,** 259–264 (1973).

5. Ballard, F. J. & Hanson, R. W. Purification of phosphoenolpyruvate carboxykinase from the cytosol fraction of rat liver and the immunochemical demonstration of differences between this enzyme and the mitochondrial phosphoenolpyruvate carboxykinase. *J. Biol. Chem.* **244,** 5625–5630 (1969).

6. Benvenisty, N., Mencher, D., Meyuhas, O., Razin, A., Reshef, L. Sequential Changes in DNA Methylation Patterns of the Rat Phosphoenolpyruvate Carboxykinase Gene during Development. *Proc. Natl. Acad. Sci.* **82,** 267–271 (2016).

7. Burgess, S. C., He, T., Yang, Z., Lindner, J., Sherry, A. D., Malloy, C. R., Browning, J. D., Magnuson, M. A. Cytosolic Phosphoenolpyruvate Carboxykinase Does Not Solely Control the Rate of Hepatic Gluconeogenesis in the Intact Mouse Liver. *Cell Metab.* **5,** 313–320 (2007).

8. DiTullio, N. W., Berkoff, C. E., Blank, B., Kostos, V., Stack, E. J., Saunders, H. L. 3-Mercaptopicolinic Acid , An Inhibitor of Gluconeogenesis. *Biochem. J.* **138,** 387–394 (1974).

9. Carlson, G. M. & Holyoak, T. Structural insights into the mechanism of phosphoenolpyruvate carboxykinase catalysis. *J. Biol. Chem.* **284,** 27037–27041 (2009).

10. Chang, H. & Lane, D. The Enzymatic Carboxylation of Phosphoenolpyruvate. *J. Biol. Chem.* **243,** 2405–2412 (1966).

11. Chiba, Y., Kamikawa, R., Nakada-Tsukui, K., Saito-Nakano, Y. & Nozaki, T. Discovery of PP-type phosphoenolpyruvate carboxykinase genes in Eukaryotes and Bacteria. *J. Biol. Chem.* **290,** 23960–23970 (2015).

12. Curthoys, N. P. & Gstraunthaler, G. Mechanism of increased renal gene expression during metabolic acidosis. *Am. J. Physiol. Renal Physiol.* **281,** 381–390 (2001).

13. Cymeryng, C., Cazzulo, J. & Cannata, J. Phosphoenolpyruvate carboxykinase from Trypanosome cruzi. Purification and physicochemical and kinetic properties. *Mol. Biochem. Parasitol.* **73,** 91–101 (1995).

14. Das, B., Ramnath, Asim Kumar, D. & Tandon, T. Differential kinetics at PK/PEPCK branch point in the cestode, Raillietina echinobothrida. *Exp. Parasitol.* **153,** 151–159 (2015).

15. DeBerardinis, R. J. *et al.* Beyond aerobic glycolysis: transformed cells can engage in glutamine

metabolism that exceeds the requirement for protein and nucleotide synthesis. *Proc. Natl. Acad. Sci.* **104,** 19345–19350 (2007).

16. Dunten, P., Belunis, C., Crowther, R., Hollfelder, K., Kammalott, U., Levin, W., Michel, H., Ramsey, G. W., Swain, A., Weber, D., Wertheimer, S. J. Crystal Structure of Human Cytosolic Phosphoenolpyruvate Carboxykinase Reveals a New GTP-binding Site. *J. Mol. Biol.* **316,** 257–264 (2002).

17. Granner, D., Andreone, T., Sasaki, K. & Beale, E. Inhibition of transcription of the phosphoenolpyruvate carboxykinase gene by insulin. *Nature* **305,** 549–551 (1983).

18. Hakimi, P., Johnson, M. T., Yang, J., Lepage, D. F., Conlon, R. A., Kalhan, S. C., Reshef, L., Tilghman, S. M., Hanson, R. W. Phosphoenolpyruvate carboxykinase and the critical role of cataplerosis in the control of hepatic metabolism. *Nutr. Metab. (Lond).* **2,** 1–12 (2005).

19. Hall, R. K., Wang, X. L., George, L., Koch, S. R. & Granner, D. K. Insulin represses phosphoenolpyruvate carboxykinase gene transcription by causing the rapid disruption of an active transcription complex: a potential epigenetic effect. *Mol. Endocrinol.* **21,** 550–563 (2007).

20. Hanson, R. & Garber, A. Phosphoenolpyruvate I. Its role in gluconeogenesis. *Am. J. Clin. Nutr.* **25,** 1010–1021 (1972).

21. Holten, D. & Nordalie, R. Comparative Studies of Catalytic Properties of Guinea Pig LIver Intra- and Extramitochondrial Phosphoenolpyruvate Carboxykinase. *Biochemistry* **4,** 201–218 (2008).

22. Holyoak, T., Sullivan, S. M. & Nowak, T. Structural Insight into the Mechanism of PEPCK Catalysis. *Biochemistry* **45,** 8254–63 (2006).

23. Jiang, W. Wang, S., Xiao, M., Lin, Y., Zhou, L., Lei, Q., Xiong, Y., Guan, K. L., Zhao, S. Acetylation regulates gluconeogenesis by promoting PEPCK1 degradation via recruiting the UBR5 ubiquitin ligase. *Mol. Cell* **43,** 33–44 (2010).

24. Johnson, T. A., Mcleod, M. J. & Holyoak, T. Utilization of Substrate Intrinsic Binding Energy for Conformational Change and Catalytic Function in Phosphoenolpyruvate Carboxykinase. *Biochemistry* **55,** 575–587 (2016).

25. Johnson, T. & Holyoak, T. The Ω-loop lid domain of phosphoenolpyruvate carboxykinase is essential for catalytic function. *Biochemistry* **51,** 9547–9559 (2012).

26. Jomain-Baum, M., Schramm, V. & Hanson, R. Mechanism of 3-Mercaptopicolinic Acid Inhibition Phosphoenolpyruvate Carboxykinase of Hepatic. *J. Biol. Chem.* **251,** 37–44 (1976).

27. Kaiser, S. & Curthoys, N. P. Effect of pH and bicarbonate on phosphoenolpyruvate carboxykinase and glutaminase mRNA levels in cultured renal epithelial cells. *J. Biol. Chem.* **266,** 9397–9402 (1991).

28. Knyphausen, P. de Boor, S., Kuhlmann, N., Scislowski, L., Extra, A., Baldus, L., Schacherl. M., Baumann, U., Neundorf, I., Lammers. M. Insights into lysine-deacetylation of natively folded substrate proteins by sirtuins. *J. Biol. Chem.* **291,** 14677–14694 (2016).

29. Lamers, W. H., Hanson, R. W. & Meisner, H. M. cAMP stimulates transcription of the gene for cytosolic phosphoenolpyruvate carboxykinase in rat liver nuclei. *Proc. Natl. Acad. Sci.* **79,** 5137–41 (1982).

30. Lee, M. H., Hebda, C. A. & Nowak, T. The role of cations in avian liver phosphoenolpyruvate carboxykinase catalysis. Activation and regulation. *J. Biol. Chem.* **256,** 12793–12801 (1981).

31. Leithner, K., Hrzenjak, A., Trotzmuller, M., Moustafa, T., Koefeler, H. C., Wohlkoenig, C., Stacher, E.,. Lindenmann, J., Harris, A. L., Olschewski, A., Olschewski, H. PCK2 activation mediates an adaptive response to glucose depletion in lung cancer. *Oncogene* **34,** 1044–1050 (2015).

32. Lewis, C. T., Seyerq, J. M. & Carlsonn, G. M. Cysteine 288 : An Essential Hyperreactive Thiol of Cytosolic Phosphoenolpyruvate Carboxykinase (GTP). *J. Biol. Chem.* **264,** 27–33 (1989).

33. Li, Y., Luo, S., Ma, R., Lui, J., Xu, P., Zhang, H, Tang, K., Ma, J., Zhang, Y., Liang, X., Sun, Y., Ji, T., Wang, N., Huang, B. Upregulation of cytosolic phosphoenolpyruvate carboxykinase is a critical metabolic event in melanoma cells that repopulate tumors. *Cancer Res.* **75,** 1191–1196 (2015).

34. Lin, Y., Lu, J. Y., Zhang, J., Walter, W., Dang, W., Wan, J., Tao, S. C., Qian, J., Zhao, Y., Boeke, J. D., Berger, S. L., Zhu, H. Protein Acetylation Microarray Reveals NuA4 Controls Key Metabolic Target Regulating Gluconeogenesis. *Cell* **136,** 1073–1084 (2010).

35. Makinen, A. & Nowak, T. 3-Mercaptopicolinate. *J. Biol. Chem.* **258,** 11654–11662 (1983).

36. Marrero, J., Rhee, K. Y., Schnappinger, D., Pethe, K. & Ehrt, S. Gluconeogenic carbon flow of tricarboxylic acid cycle intermediates is critical for Mycobacterium tuberculosis to establish and maintain infection. *Proc. Natl. Acad. Sci. U. S. A.* **107,** 9819–9824 (2010).

37. Matte, A., Goldie, H., Sweet, R. M. & Delbaere, L. T. Crystal structure of Escherichia coli phosphoenolpyruvate carboxykinase: a new structural family with the P-loop nucleoside triphosphate hydrolase fold. *J. Mol. Biol.* **256,** 126–143 (1996).

38. Méndez-lucas, A., Duarte, J., Sunny, N. E., Satapati, S., He, T., Fu, X., Bermudez, J., Burgess, S. C., Perales, J. C. PEPCK-M expression in mouse liver potentiates, not replaces, PEPCK-C mediated gluconeogenesis. *J. Hepatol.* **59,** 105–113 (2014).

39. Mendez-Lucas, A., Hyrossova, P., Novellasdemunt, L., Vinals, F. & Perales, J. Mitochondrial phosphoenolpyruvate carboxykinase (PEPCK-M) is a pro-survival, endoplasmic reticulum (ER) stress response gene involved in tumor cell adaptation to nutrient availability. *J. Biol. Chem.* **289,** 22090–22102 (2014).

40. Modaressi, S., Brechtel, K., Christ, B. & Jungermann, K. Human mitochondrial phosphoenolpyruvate carboxykinase 2 gene. Structure, chromosomal localization and tissue-specific expression. *Biochem. J.* **333,** 359–66 (1998).

41. Nordlie, R. C., Lardy, H. A. Mammalian Liver Phosphoenolpyruvate Carboxykinase Activities. *J. Biol. Chem.* ***238,*** 2259-2263 (1963).

42. Park, J. W. Kim, S. C., Kim, W. K., Hong, J. P., Kim, K-H., Yeo, H. Y., Lee, J. Y., Kim, M. S., Kim, J. H., Yang, S. Y., Kim. D. Y., Oh, J. W., Cho, J. Y., Yoo, Y. C. Expression of phosphoenolpyruvate carboxykinase linked to chemoradiation susceptibility of human colon cancer cells. *BMC Cancer* **14,** 1–12 (2014).

43. Pérez, E., Espinoza, R., Laiveniekcs, M. & Cardemil, E. Stereochemistry of the carboxylation reaction catalyzed by the ATP-dependent phosphoenolpyruvate carboxykinases from Saccharomyces cerevisiae and Anaerobiospirillum succiniciproducens. *Biochimie* **90,** 1685–1692 (2008).

44. Pollock, A. S. & Long, J. A. The 5' region of the rat phosphoenolpyruvate carboxykinase gene confers pH sensitivity to chimeric genes expressed in renal and liver cell lines capable of expressing PEPCK. *Biochem. Biophys. Res. Commun.* **164,** 81–87 (1989).

45. Ray, P. D. & Lardy, A. Paths of Carbon in Gluconeogenesis Lipogenesis. *J. Biol. Chem.* **241,** 3904–3908 (1966).

46. Reshef, L. & Hanson, R. The Interaction of Catecholamines and Adrenal Corticosteroids in the Induction of Phosphopyruvate Carboxylase in Rat Liver and Adipose Tissue. *Biochem. J.* **127,** 809–818 (1972).

47. Robinson, B. H. & Oei, J. 3-Mercaptopicolinic acid, a preferential inhibitor of the cytosolic phosphoenolpyruvate carboxykinase. *FEBS Lett.* **58,** 12–15 (1975).

48. Seenappa, V., Das, B., Joshi, M. B., Satyamoorthy, K. Context Depependent Regulation of Human Phosphoenolpyruvate Carboxykinase Isoforms by DNA Promoter Methylation and RNA Stability. *J. Cell. Biochem.* **9999,** 1-15 (2016).

49. She, P., Shiota, M., Shelton, K. D., Chalkey, R., Postic, C., Magnuson, M. A. Phosphoenolpyruvate carboxykinase is necessary for the integration of hepatic energy metabolism. *Mol. Cell. Biol.* **20,** 6508–6517 (2000).

50. Snoke, R. E., Johnston, J. B. & Lardy, H. A. Response of phosphopyruvate carboxylase to tryptophan metabolites and metal ions. *Eur. J. Biochem.* **24,** 342–346 (1971).

51. Stark, R., Guebre-Egziabher, F., Zhao, X., Feriod, C., Dong, J., Alves, T. C., Loja, S., Pongratz, R. L., Bhanot, S., Roden, M., Cline, G. C., Shulman, G. I., Kibbey, R. G. A role for mitochondrial phosphoenolpyruvate carboxykinase (PEPCK-M) in the regulation of hepatic gluconeogenesis. *J. Biol. Chem.* **289,** 7257–7263 (2014).

52. Stark, R. & Kibbey, R. G. The mitochondrial isoform of phosphoenolpyruvate carboxykinase (PEPCK-M) and glucose homeostasis: Has it been overlooked? *Biochim. Biophys. Acta* **1840,** 1313–1330 (2014).

53. Stark, R., Pazquel, F., Turcu, A., Pongratz, R. L., Roden, Mo., Cline, G. W., Shulman, G. I., Kibbey, R. G. Phosphoenolpyruvate cycling via mitochondrial phosphoenolpyruvate carboxykinase links anaplerosis and mitochondrial GTP with insulin secretion. *J. Biol. Chem.* **284,** 26578–26590 (2009).

54. Stiffin, R. M., Sullivan, S. M., Carlson, G. M. & Holyoak, T. Differential inhibition of cytosolic PEPCK by substrate analogues. Kinetic and structural characterization of inhibitor recognition. *Biochemistry* **47,** 2099–2109 (2008).

55. Stiffin, R. M., Sullivan, S. M., Carlson, G. M. & Holyoak, T. Inhibitor scaffold for the inhibition of the enzyme phosphoenolpyruvate carboxykinase. US Patent 12/834,609. Jul 12, 2010.

56. Sugden, M. C. & Ashcroft, S. J. H. Phosphoenolpyruvate in rat pancreatic islets: A possible intracellular trigger of insulin release? *Diabetologia* **13,** 481–486 (1977).

57. Sullivan, S. M. & Holyoak, T. Structures of rat cytosolic PEPCK: Insight into the mechanism of phosphorylation and decarboxylation of oxaloacetic acid. *Biochemistry* **46,** 10078–88 (2007).

58. Sulllivan, S. M. & Holyoak, T. Enzymes with lid-gated active sites must operate by an induced fit

mechanims instead of confromational selection. *Proc. Natl. Acad. Sci* **105**, 13829-13834 (2008).

59. Szollosi, A., Nenquin, M., Aguilar-Bryan, L., Bryan, J. & Henquin, J.-C. Glucose stimulates Ca2+ influx and insulin secretion in 2-week-old beta-cells lacking ATP-sensitive K+ channels. *J. Biol. Chem.* **282,** 1747–1756 (2007).

60. Tilghman, S. M., Hanson, R. W., Reshef, L., Hopgood, M. F. & Ballard, F. J. Rapid loss of translatable messenger RNA of phosphoenolpyruvate carboxykinase during glucose repression in liver. *Proc. Natl. Acad. Sci.* **71,** 1304–1308 (1974).

61. Traut, T. W. The functions and consensus motifs of nine types of peptide segments that form different types of nucleotide-binding sites. *Eur. J. Biochem.* **222,** 9–19 (1994).

62. Utter, M. F. & Kurahashi, K. Mechanism of action of Oxalacetic Carboxylase. *J. Biol. Chem.* **207,** 821–841 (1954).

63. Veneziale, C. M., Walter, P., Kneer, N. & Lardy, H. A. Influence of L-Tryptophan and Its Metabolites on Gluconeogenesis in the Isolated, Perfused Liver. *Biochemistry* **6,** 2129–2138 (1967).

64. Vincent, E. E., Sergushichev, A., Griss, T., Gingras, M. C., Samborska, B., Ntimbane, T., Coelho, P. P., Blagih, J., Raissi, T. C., Choiniere, L., Bridon, G., Loginicheva, E., Flynn, B. R., Thomas, E. C., Tavare, J. M., Avizonis, D., Pause, A., Elder, D., Artyomov, M. N., Jones, R. G. Mitochondrial Phosphoenolpyruvate Carboxykinase Regulates Metabolic Adaptation and Enables Glucose-Independent Tumor Growth. *Mol. Cell* **60,** 195–207 (2015).

65. Warburg, O., Wind, F., Negelein, E. The metabolism of tumors in the body. *J. Gen. Physiol.* **182,** 519–530 (1926).

66. Williams, C. P., Postic C., Robin, D., Robin, P., Parrinello, J., Shelton, K., Printz, R. L., Magnuson, M. A., Granner, D. K., Forest, C., Chalkley, R. Isolation and characterization of the mouse cytosolic phosphoenolpyruvate carboxykinase (GTP) gene: Evidence for tissue-specific hypersensitive sites. *Mol. Cell. Endocrinol.* **148,** 67–77 (1999).

67. Yuan, Y., Hakimi, P., Kao, C., Kao, A., Lui, R., Janocha, A., Boyd-Tressler, A., Hang, x., Alhoraibi, H., Slater, E., Xia, K., Cao, P., Shue, Q., Ching, T-T., Hsu, A., Erzurum, S. C., Dubyak, G. R., Berger, N. A., Hanson, R. W., Feng, Z. Reciprocal changes in phosphoenolpyruvate carboxykinase and pyruvate kinase with age are a determinant of aging in Caenorhabditis elegans. *J. Biol. Chem.* **291,** 1307–1319 (2016).

Appendix:

Equations:

$$\Delta G = -RTlnKi = \Delta H - T\Delta S$$

Equation 12.1 – Gibbs free energy. ΔG is change in free energy, R is ideal gas constant, T is temperature, K_i is inhibition constant, ΔH is change in enthalpy, and ΔS is change in entropy.

$$y = min + \frac{(max - min)}{1 + \frac{x}{IC50}}$$

Equation 12.2 – Determination of $IC_{50.}$ Min and max are taken from experimental graph. Y and X are variables.

$$Ki = \frac{IC50}{1 + \frac{[S]}{Km}}$$

Equation 12.3 – Determination of K_i from IC_{50} values to fit competitive model. [S] is substrate concentration, and K_m is Michaelis binding constant

$$v = \frac{Vmax}{1 + (\frac{Km}{[S]})(1 + \frac{[I]}{Ki})}$$

Equation 12.4 – Fit to competitive model. V_{max} is maximal velocity, and [I] is inhibitor concentration.

$$\boldsymbol{v} = \frac{\boldsymbol{Vmax}[\boldsymbol{S}]}{\boldsymbol{Km} + [\boldsymbol{S}]}$$

Equation 12.5 – Michaelis menten equation.

Inhibition of Rat Cytosolic PEPCK by CMP Fit To Competive Inhibition Model

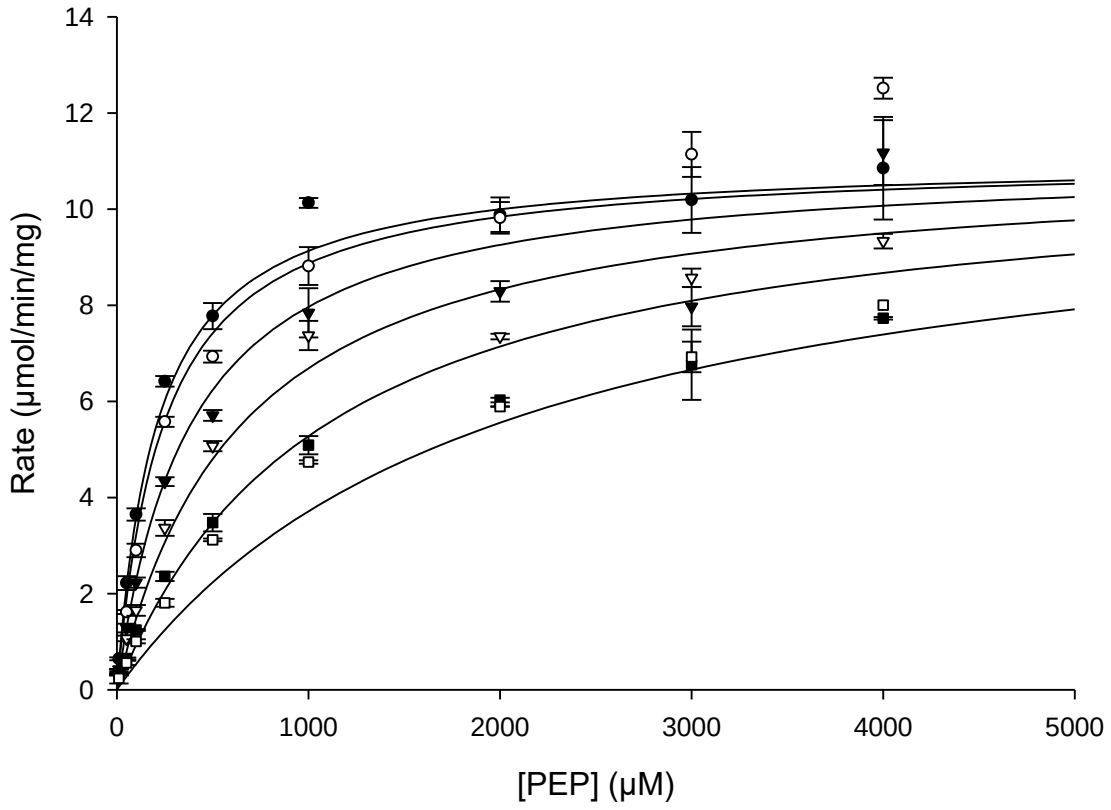

V_{max} = 11.0umol/min/mg

K_m = 208.8uM

K_i = 11.8uM

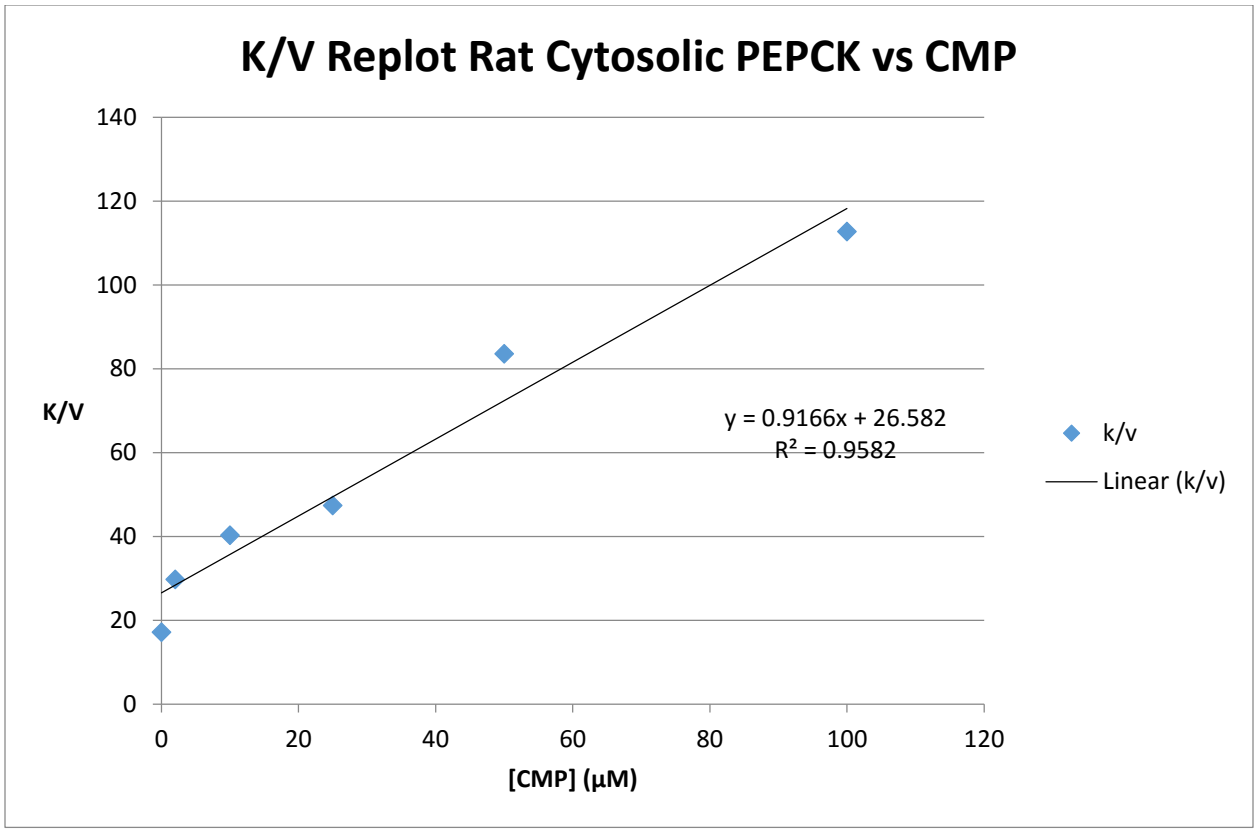
K/V Replot Rat Cytosolic PEPCK vs CMP
140
120
100
80
60
40
20
0
K/V
0
20
40
60
80
100
120
[CMP] (µM)
y = 0.9166x + 26.582
R² = 0.9582
k/v
Linear (k/v)

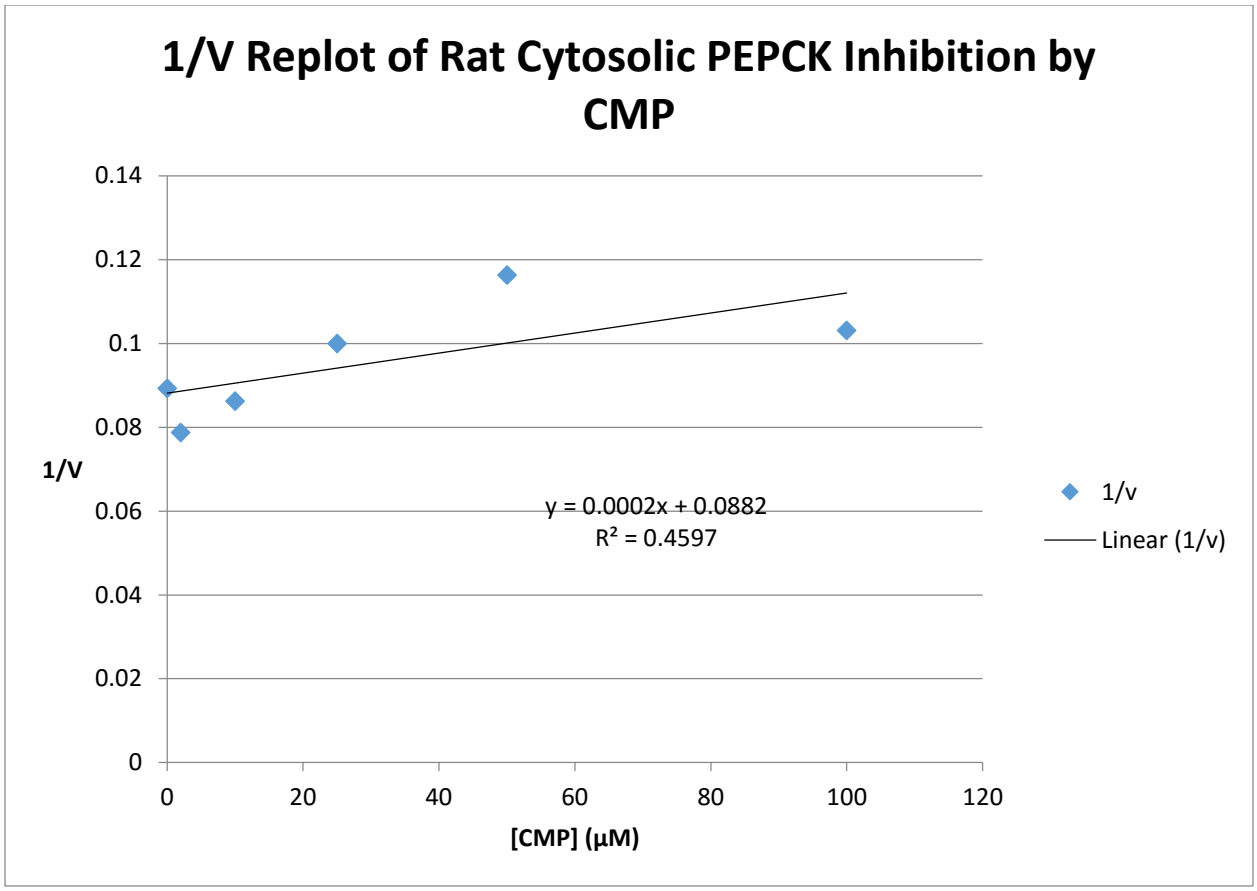
1/V Replot of Rat Cytosolic PEPCK Inhibition by CMP
0.14
0.12
0.1
0.08
0.06
0.04
0.02
0
1/V
0
20
40
60
80
100
120
[CMP] (µM)
y = 0.0002x + 0.0882
R² = 0.4597
1/v
Linear (1/v)

Inhibition of Mycobacterium Tuberculosis PEPCK by CMP Fit To Competive Inhibition Model

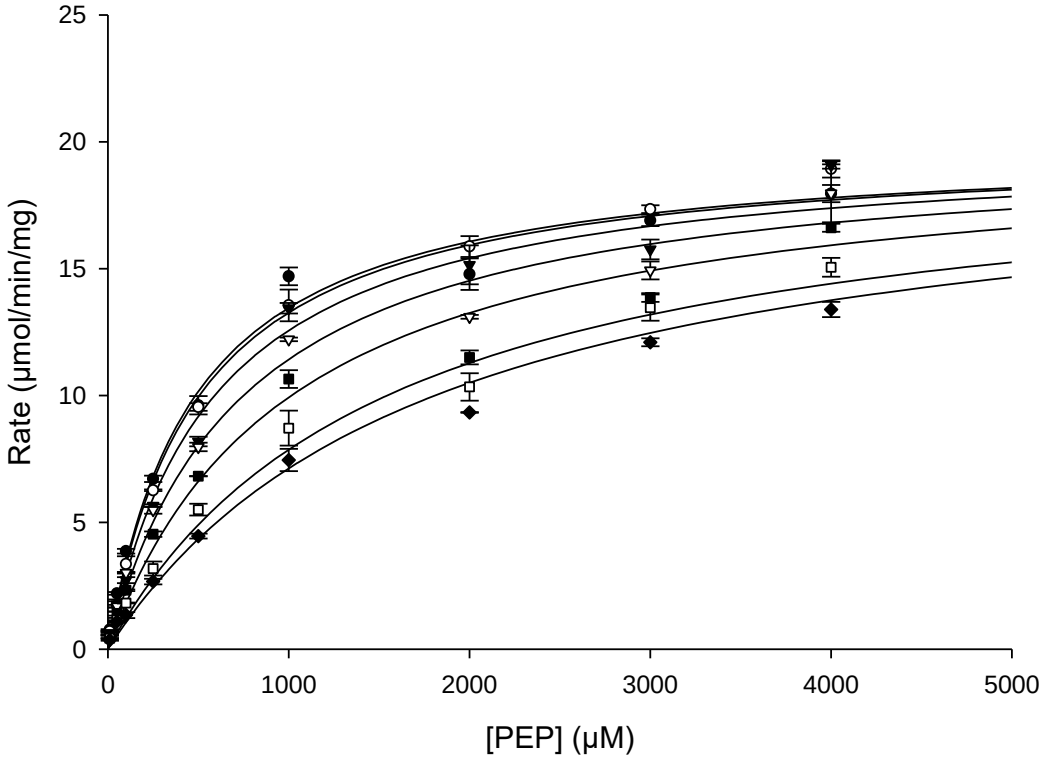

V_{max} = 19.9umol/min/mg

K_m = 481.7uM

K_i = 45.7uM

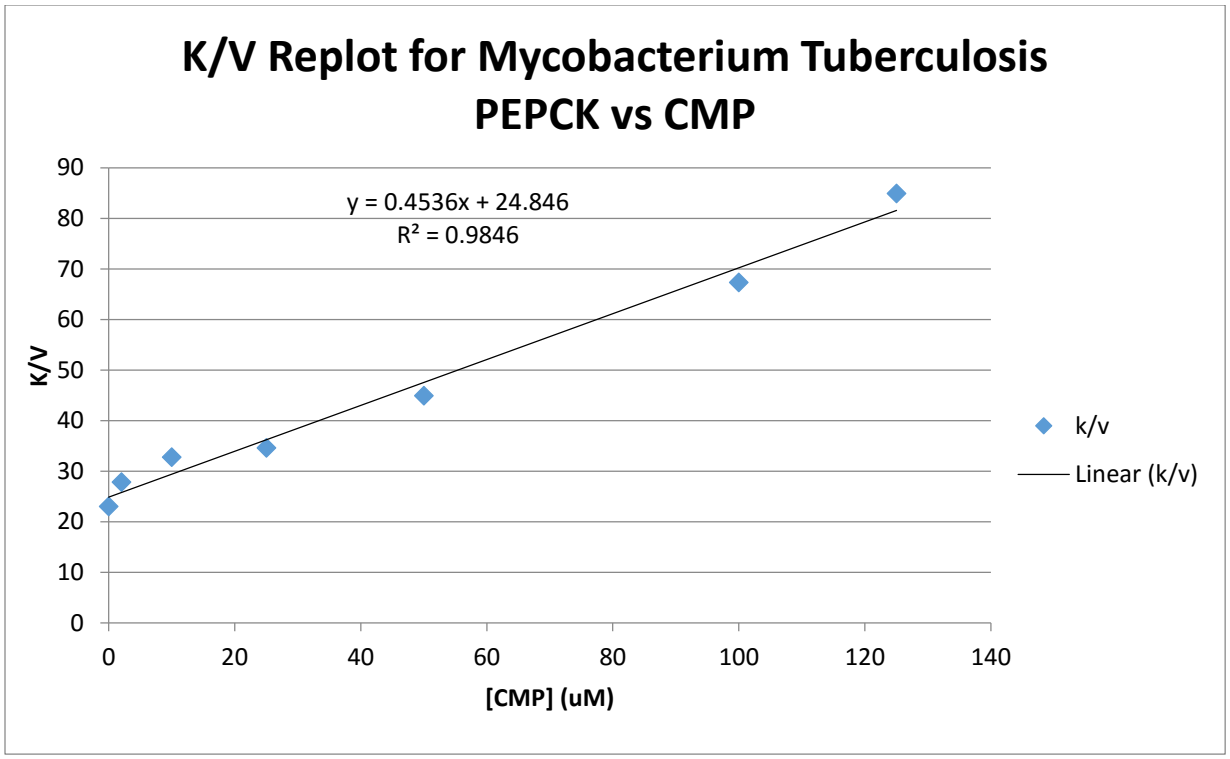
K/V Replot for Mycobacterium Tuberculosis
PEPCK vs CMP
y = 0.4536x + 24.846
R² = 0.9846
K/V
[CMP] (uM)
k/v
Linear (k/v)
0
10
20
30
40
50
60
70
80
90
0
20
40
60
80
100
120
140

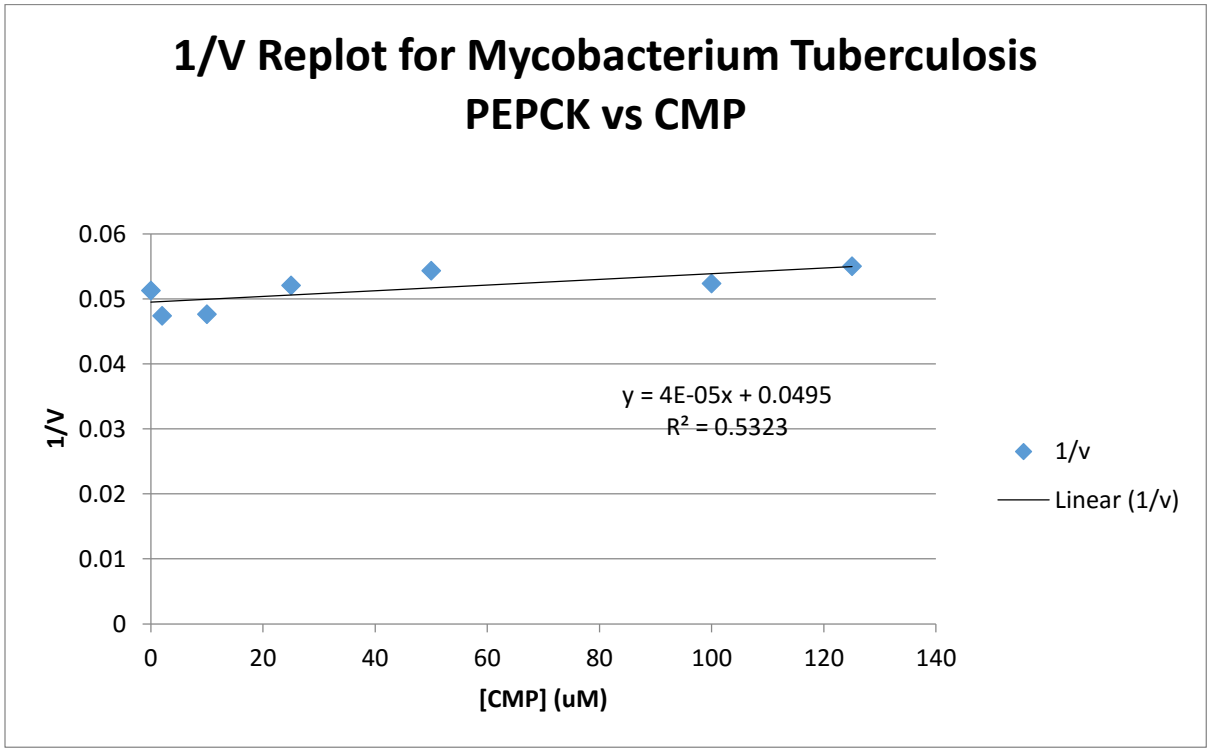
1/V Replot for Mycobacterium Tuberculosis
PEPCK vs CMP
0.06
0.05
0.04
0.03
0.02
0.01
0
1/V
y = 4E-05x + 0.0495
R² = 0.5323
0
20
40
60
80
100
120
140
[CMP] (uM)
1/v
Linear (1/v)

Inhibition of Human Mitochondrial PEPCK by CMP Fitted to Competitive Model

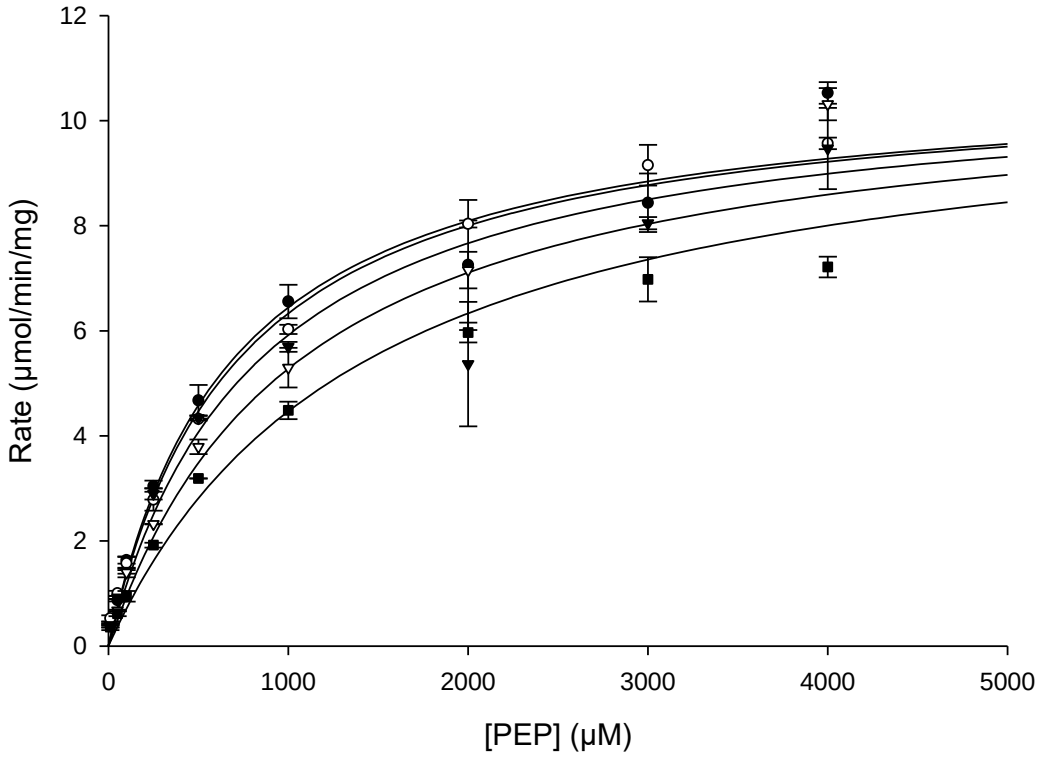

V_{max} = 10.9umol/min/mg

K_m = 686.0uM

K_i = 46.0uM

● I = 0
○ I = 2
▼ I = 10
▽ I = 25
■ I = 50

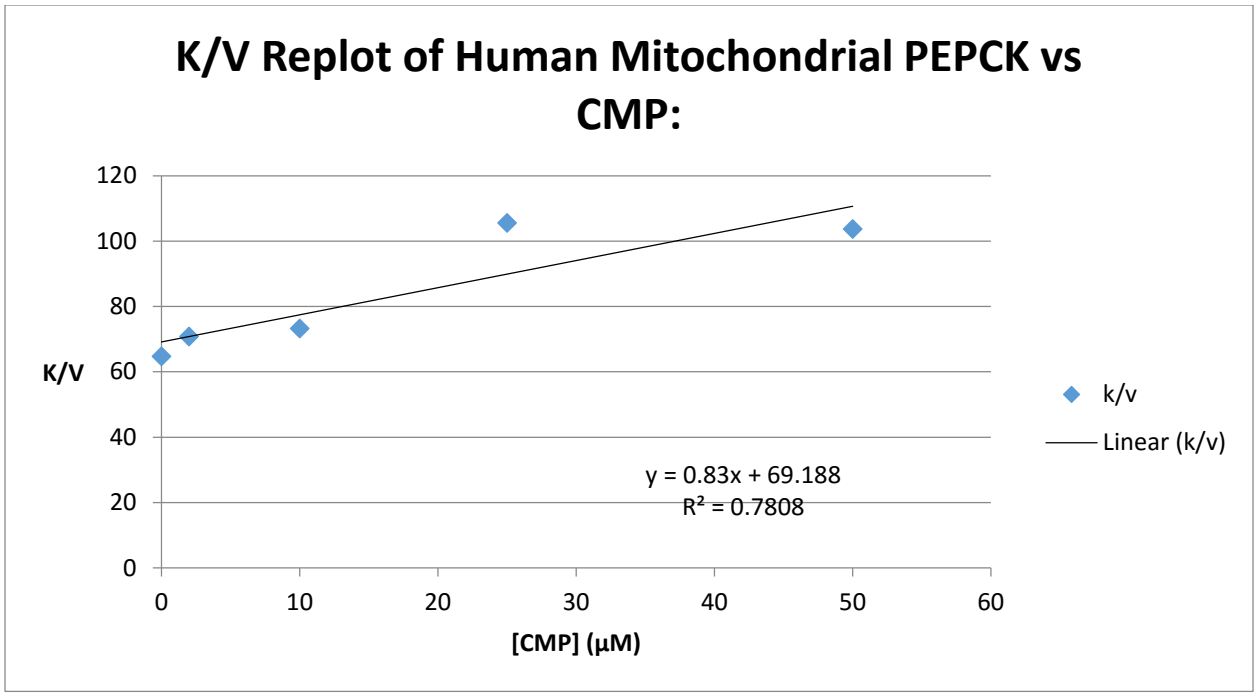
K/V Replot of Human Mitochondrial PEPCK vs CMP:
120
100
80
60
40
20
0
K/V
0
10
20
30
40
50
60
[CMP] (µM)
y = 0.83x + 69.188
R² = 0.7808
k/v
Linear (k/v)

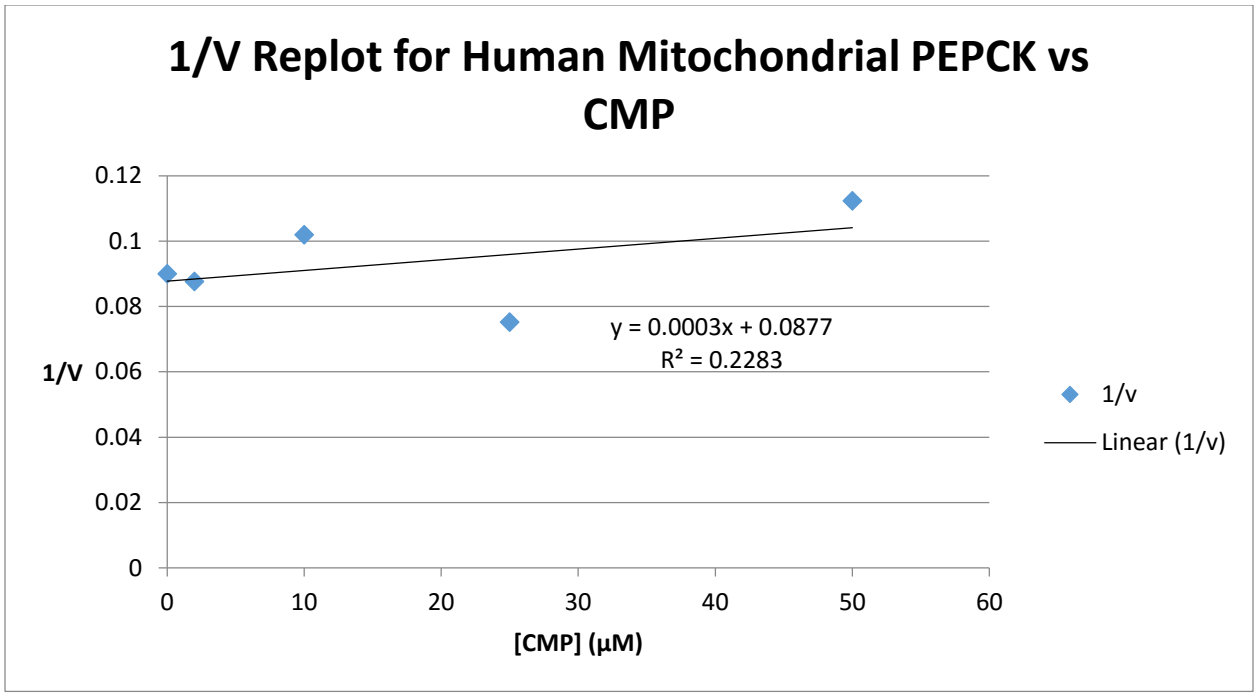
1/V Replot for Human Mitochondrial PEPCK vs CMP
0.12
0.1
0.08
0.06
0.04
0.02
0
1/V
0
10
20
30
40
50
60
[CMP] (µM)
y = 0.0003x + 0.0877
R² = 0.2283
1/v
Linear (1/v)

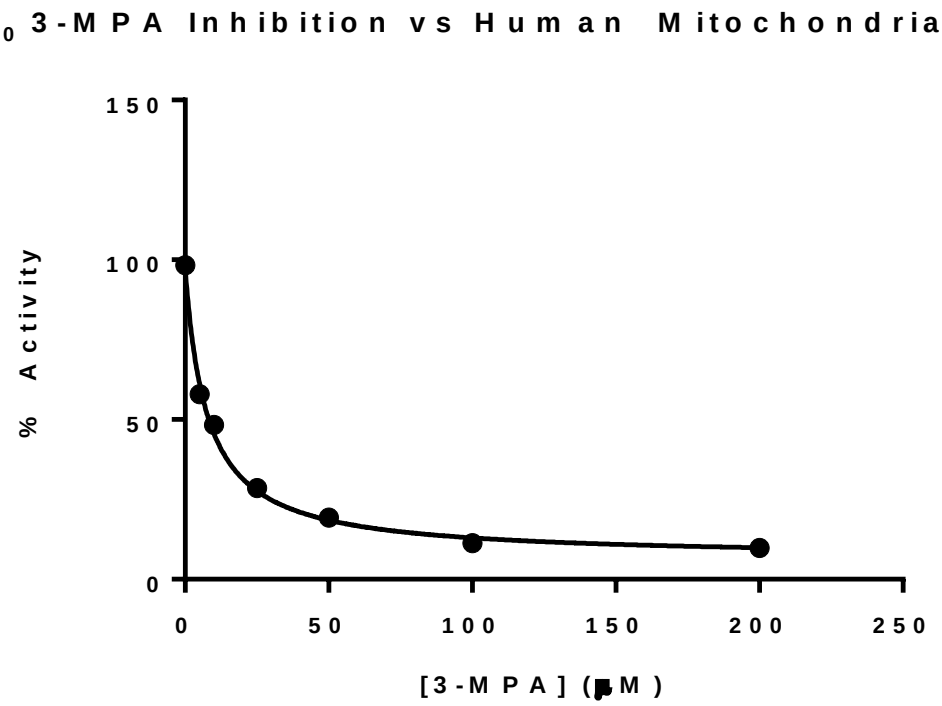

Errors bars are hidden within data points for all IC_{50} inhibition curves

IC_{50} CMP Inhibition vs Human Mitochondrial PEPCK

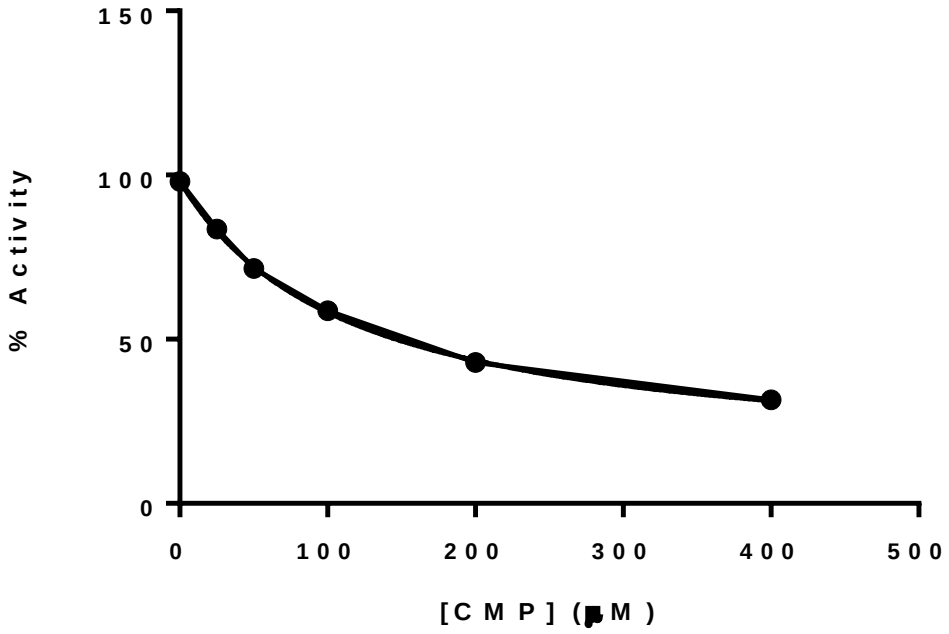

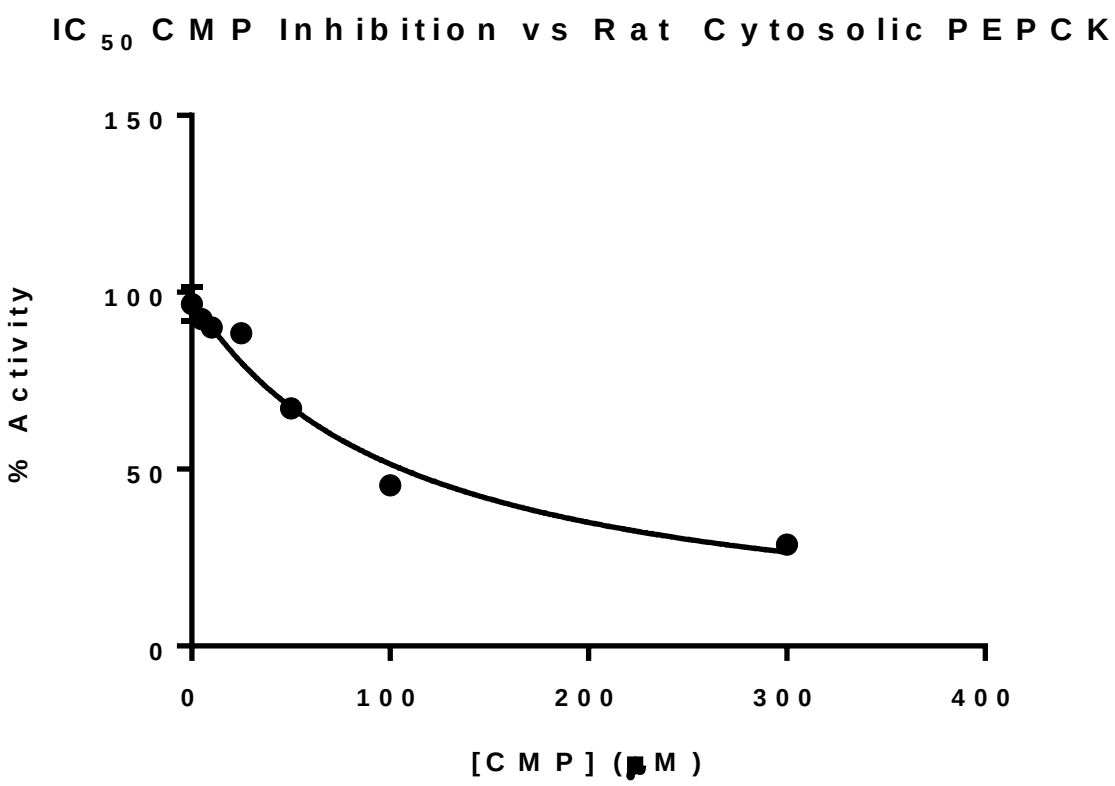
IC50 CMP Inhibition vs Rat Cytosolic PEPCK
150
100
50
0
% Activity
0
100
200
300
400
[CMP] (μM)

	rcPEPCK_CMP
Wavelength (Å)	0.97952
Space Group	$P2_1$
Unit Cell	*a*=44.4 Å
	b=118.7 Å
	c=60.4 Å
	α=γ=90 Å
	β=109.6 Å
Resolution Limits	59.53-1.49 Å
No. of Unique Reflection	158815
Completeness	99.9 %
Redundancy	4.8 (4.6)
I/Iσ(I)	20.5 (2.5)
Rmerge	0.08 (0.5)
REFINEMENT	
Resolution Limits (Å)	59.35-1.49
No. of ASU Molecules	1
R_{free}	0.177 (0.279)
R_{work}	0.153 (0.281)
Average B Factor (Å^2) - Protein	23.9
Metals	22.8
CMP	21.2
Water	33.7
Estimated Coordinate Error Based on Maximum Likelihood (Å)	0.048
Bond Length Root-Mean-Square Deviation (Å)	0.02
Bond Angle Room-Mean-Square Deviation (°)	2.23
Molprobity Statistics - Score	1.09
Percentile	99th
No. of Ramachandran Outliers	2

*Highest resolution shell data in parentheses – 1.49-1.55Å *